

**This is an electronic reprint of the original article.**

**This reprint *may differ* from the original in pagination and typographic detail.**

**Author(s):** Ze-Hui Chen, Ya-Xi Xu, Xing-Long Xie, Dong-Feng Wang, Diana Aguilar-Gómez, Guang-Jian Liu, Xin Li, Ali Esmailizadeh, Vahideh Rezaei, Juha Kantanen, Innokentyi Ammosov, Maryam Nosrati, Kathiravan Periasamy, David W. Coltman, Johannes A. Lenstra, Rasmus Nielsen & Meng-Hua Li

**Title:** Whole-genome sequence analysis unveils different origins of European and Asiatic mouflon and domestication-related genes in sheep

**Year:** 2021

**Version:** Published version

**Copyright:** The Author(s) 2021

**Rights:** CC BY 4.0

**Rights url:** <http://creativecommons.org/licenses/by/4.0/>

**Please cite the original version:**

Chen, ZH., Xu, YX., Xie, XL. et al. Whole-genome sequence analysis unveils different origins of European and Asiatic mouflon and domestication-related genes in sheep. *Commun Biol* 4, 1307 (2021). <https://doi.org/10.1038/s42003-021-02817-4>

All material supplied via *Jukuri* is protected by copyright and other intellectual property rights. Duplication or sale, in electronic or print form, of any part of the repository collections is prohibited. Making electronic or print copies of the material is permitted only for your own personal use or for educational purposes. For other purposes, this article may be used in accordance with the publisher's terms. There may be differences between this version and the publisher's version. You are advised to cite the publisher's version.

## Whole-genome sequence analysis unveils different origins of European and Asiatic mouflon and domestication-related genes in sheep

Ze-Hui Chen<sup>1,2,3,16</sup>, Ya-Xi Xu<sup>3,16</sup>, Xing-Long Xie<sup>1,2</sup>, Dong-Feng Wang<sup>1,2</sup>, Diana Aguilar-Gómez<sup>4</sup>, Guang-Jian Liu<sup>5</sup>, Xin Li<sup>1,2</sup>, Ali Esmailzadeh<sup>6</sup>, Vahideh Rezaei<sup>6</sup>, Juha Kantanen<sup>7</sup>, Innokentyi Ammosov<sup>8</sup>, Maryam Nosrati<sup>9</sup>, Kathiravan Periasamy<sup>10</sup>, David W. Coltman<sup>11</sup>, Johannes A. Lenstra<sup>12</sup>, Rasmus Nielsen<sup>13,14,15</sup>✉ & Meng-Hua Li<sup>3</sup>✉

The domestication and subsequent development of sheep are crucial events in the history of human civilization and the agricultural revolution. However, the impact of interspecific introgression on the genomic regions under domestication and subsequent selection remains unclear. Here, we analyze the whole genomes of domestic sheep and their wild relative species. We found introgression from wild sheep such as the snow sheep and its American relatives (bighorn and thinhorn sheep) into urial, Asiatic and European mouflons. We observed independent events of adaptive introgression from wild sheep into the Asiatic and European mouflons, as well as shared introgressed regions from both snow sheep and argali into Asiatic mouflon before or during the domestication process. We revealed European mouflons might arise through hybridization events between a now extinct sheep in Europe and feral domesticated sheep around 6000–5000 years BP. We also unveiled later introgressions from wild sheep to their sympatric domestic sheep after domestication. Several of the introgression events contain loci with candidate domestication genes (e.g., *PAPPA2*, *NR6A1*, *SH3GL3*, *RFX3* and *CAMK4*), associated with morphological, immune, reproduction or production traits (wool/meat/milk). We also detected introgression events that introduced genes related to nervous response (*NEURL1*), neurogenesis (*PRUNE2*), hearing ability (*USH2A*), and placental viability (*PAG11* and *PAG3*) into domestic sheep and their ancestral wild species from other wild species.

<sup>1</sup>CAS Key Laboratory of Animal Ecology and Conservation Biology, Institute of Zoology, Chinese Academy of Sciences (CAS), Beijing, China. <sup>2</sup>University of Chinese Academy of Sciences (UCAS), Beijing, China. <sup>3</sup>College of Animal Science and Technology, China Agricultural University, Beijing, China. <sup>4</sup>Center for Computational Biology, University of California at Berkeley, Berkeley, CA 94720, USA. <sup>5</sup>Novogene Co., Ltd, Tianjin, China. <sup>6</sup>Department of Animal Science, Faculty of Agriculture, Shahid Bahonar University of Kerman, Kerman, Iran. <sup>7</sup>Natural Resources Institute Finland (Luke), Jokioinen, Finland. <sup>8</sup>Laboratory of Reindeer Husbandry and Traditional Industries, Yakut Scientific Research Institute of Agriculture, The Sakha Republic (Yakutia), Yakutsk, Russia. <sup>9</sup>Department of Agriculture, Payame Noor University, Tehran, Iran. <sup>10</sup>Animal Production and Health Laboratory, Joint FAO/IAEA Division of Nuclear Techniques in Food and Agriculture, International Atomic Energy Agency, Vienna, Austria. <sup>11</sup>Department of Biological Sciences, University of Alberta, Edmonton, AB T6G2E9, Canada. <sup>12</sup>Faculty of Veterinary Medicine, Utrecht University, Utrecht, the Netherlands. <sup>13</sup>Department of Integrative Biology, University of California at Berkeley, Berkeley, CA 94720, USA. <sup>14</sup>Department of Statistics, UC Berkeley, Berkeley, CA 94707, USA. <sup>15</sup>Globe Institute, University of Copenhagen, 1350 København K, Denmark. <sup>16</sup>These authors contributed equally: Ze-Hui Chen, Ya-Xi Xu. ✉email: [rasmus\\_nielsen@berkeley.edu](mailto:rasmus_nielsen@berkeley.edu); [menghua.li@cau.edu.cn](mailto:menghua.li@cau.edu.cn)

The genus *Ovis* spans ~8.31 million years of evolution and comprises eight extant species: domestic sheep *O. aries*, argali *O. ammon*, Asiatic mouflon *O. orientalis*, European mouflon *O. musimon*, urial *O. vignei*, bighorn sheep *O. canadensis*, thinhorn sheep *O. dalli* and snow sheep *O. nivicola*<sup>1</sup>. Earlier archeological and genetic studies have provided strong evidence that sheep have been domesticated from their wild ancestor Asiatic mouflon in the Fertile Crescent ~12,000–10,000 years BP<sup>2–4</sup>. The domestication during the Neolithic agricultural revolution had contributed significantly to human civilization by providing a stable source of meat, wool, leather, and dairy.

In spite of varying diploid number of chromosomes ( $2n = 52–58$ )<sup>1</sup>, hybridization between wild and domestic sheep, as well as between wild sheep species, has been documented to produce viable and fertile interspecific hybrids<sup>5–9</sup>. Previous studies have shown genetic evidence for introgression<sup>10–14</sup>, including adaptive introgression from wild relatives to domestic sheep<sup>15,16</sup>. However, the importance of introgression in the entire *Ovis* genus and its contribution to the sheep domestication process remains largely unexplored.

Because wild sheep have adapted to different biogeographic ranges resulting in them being resilient to many biotic and abiotic stresses, the existing genetic variation of wild sheep provides an important genetic resource for improving domestic sheep in response to increased food production demands, animal disease occurrence and rapid global climate change. Elucidating the evolutionary and genetic connection between wild and domesticated sheep is therefore important for understanding the potential for using wild sheep genetic material for the improvement of domesticated sheep.

In this study, we used high-depth whole-genome sequences (average coverage = ~21×) of 72 individuals from the eight *Ovis* species, most of which were understudied in previous genomic studies<sup>7,17–19</sup>. We reconstructed the phylogeny and evolutionary history of these species. In addition, we explored gene flow between species and selection signatures of domestication. These findings added to our understanding of the origins of the Asiatic and European mouflons and the emergence of domestic sheep.

## Results

**Sequencing and variant calling.** High-depth resequencing of 72 individuals from eight *Ovis* species (Fig. 1a and Supplementary Data 1) generated a total of 35.91 billion 150-bp paired-end reads (5.39 Tb), and 35.84 billion clean reads (5.28 Tb) with an average depth of 20.7× (12.2–36.9×) per individual and average genome coverage of 97.2% (96.5%–98.3%) after filtering. The average sequence coverage was 19.3× for *O. aries*, 17.8× for *O. ammon*, 18.9× for *O. canadensis*, 19.8× for *O. vignei*, 18.9× for *O. musimon*, 17.8× for *O. nivicola*, 19.4× for *O. dalli*, and 27.1× for *O. orientalis*. On average, 95.83% individuals had ≥4× coverage, 90.11% had ≥10× coverage, and 46.68% had ≥20× coverage. Of all the individual sequencing reads, 91.86% were mapped to the *O. aries* reference genome Oar\_v4.0 (Supplementary Data 1). Summed over all samples, 125,982,209 SNPs, 13,043,920 INDELS (insertions and deletions ≤50 bp; ~0.89 million common indels shared by all sheep species and on average 2,605,718 per individual) (Table 1, Supplementary Tables 1–3, and Supplementary Data 1, 2) and a large number of genome-wide structural variations (SVs, 51 bp–997.369 kb: inversions, insertions, deletions, duplications, and translocations, on average 41,965 per individual), including copy number variations (CNVs, deletions, and duplications of 51 bp to 997.369 kb, on average 31,124 per individual) (Supplementary Data 2) were detected. The number of SVs shared by two species ranged from 29,884 to 91,186 (Supplementary Table 4 and Supplementary Fig. 1a). On average, 1.88% SVs were located in

exonic regions, 65.2% SVs were located in intergenic regions, and 29.9% SVs were located in intronic regions, while 67.0%, 31.0%, and 0.66% SNPs were in intergenic, intronic, and exonic regions, respectively (Supplementary Tables 5 and 6).

The percentage of SNPs that was present in public databases [e.g., NCBI sheep dbSNP database v150 and European Variation Archive (EVA)] ranges from 78.1% in argali to 94.3% in domestic sheep (Supplementary Data 3). Our data set added 2,139,962 novel SNPs (an increase of 7.04%) to the NCBI and EVA database of sheep genetic variants (Supplementary Data 2). Of the 176,403 common sites between detected SNPs and the Ovine BeadChip, an average of 288,638 genotypes observed here were validated by the Ovine Infinium HD SNP BeadChip data available for 14 individuals of the samples sequenced (97.1% validation rate, and 297,115 common SNPs), and an average of 23,220 genotypes was validated by the Ovine SNP50K BeadChip data available for another 12 individuals of the samples (96.64% validation rate, and 22,583 common SNPs) (Supplementary Data 3).

Moreover, 74 randomly selected SNPs, which are from the NCBI sheep dbSNP database and the candidate genes identified below, were inspected in 4–12 individuals by Sanger sequencing and produced an overall validation rate of 95.5% (Supplementary Data 3). For PCR and qPCR validation of CNVs (deletions and duplications), 14 randomly selected CNVs with 85.4% concordant genotypes (38/42 deletions and 32/40 duplications; Supplementary Data 3 and Supplementary Fig. 2) were successfully validated. The validation rates observed here are higher than those in previous studies<sup>17,20</sup>, which could be due to more efficient and precise CNV detection methods used here. The high validation rate indicated high reliability of the genetic variants created in this study.

**Patterns of variation.** The 126 million SNPs were detected across all the eight species. The number of SNPs varied from 11.3 to 20.1 million per individual and from 13.4 to 53.6 million (0.6–18.2 unique) per species (Supplementary Data 1, Supplementary Data 2, and Supplementary Fig. 3c). We observed 4,431,063 SNPs shared among all the eight species, with the shared SNPs for pairwise comparisons varying from 6,241,176 between European mouflon and snow sheep to 25,195,033 between Asiatic mouflon and urial (Supplementary Table 2 and Supplementary Data 2). More comparisons of structural variants (SVs) and copy number variants (CNVs) among species for uniqueness and sharing are shown in Supplementary Fig. 1c.

Using pairwise genome-wide  $F_{ST}$ , the species with the highest genetic differentiation between were snow sheep and European mouflon, and the ones with the least differentiation between were urial and Asiatic mouflon (Supplementary Table 7). The species with the highest genomic diversity ( $\pi$ ), when only including SNPs with <10% missing data, were domestic sheep, Asiatic mouflon, and urial (0.0032–0.0044), and the ones with the lowest diversity were snow sheep, bighorn sheep and thinhorn sheep (0.00075–0.00078) (Supplementary Fig. 4b). On average, 67.0% of SNPs were located in intergenic regions, 31.0% in introns, and 0.7% SNPs in exons. The ratio of non-synonymous to synonymous substitutions ranged from 0.72 in urial and 0.77 in domestic sheep to 0.88 in European mouflon (Supplementary Table 6). We pooled the SVs and CNVs across all the eight species yielding a high depth of coverage for the shared and unique SVs and CNVs among them (Supplementary Fig. 1a, b and Supplementary Data 2, see Supplementary Information). Annotation of genes overlapped with SVs was summarized in Supplementary Data 2.

**Phylogenomic reconstruction among the *Ovis* species.** We generated eight high-depth whole pseudo-haploid genomes (see

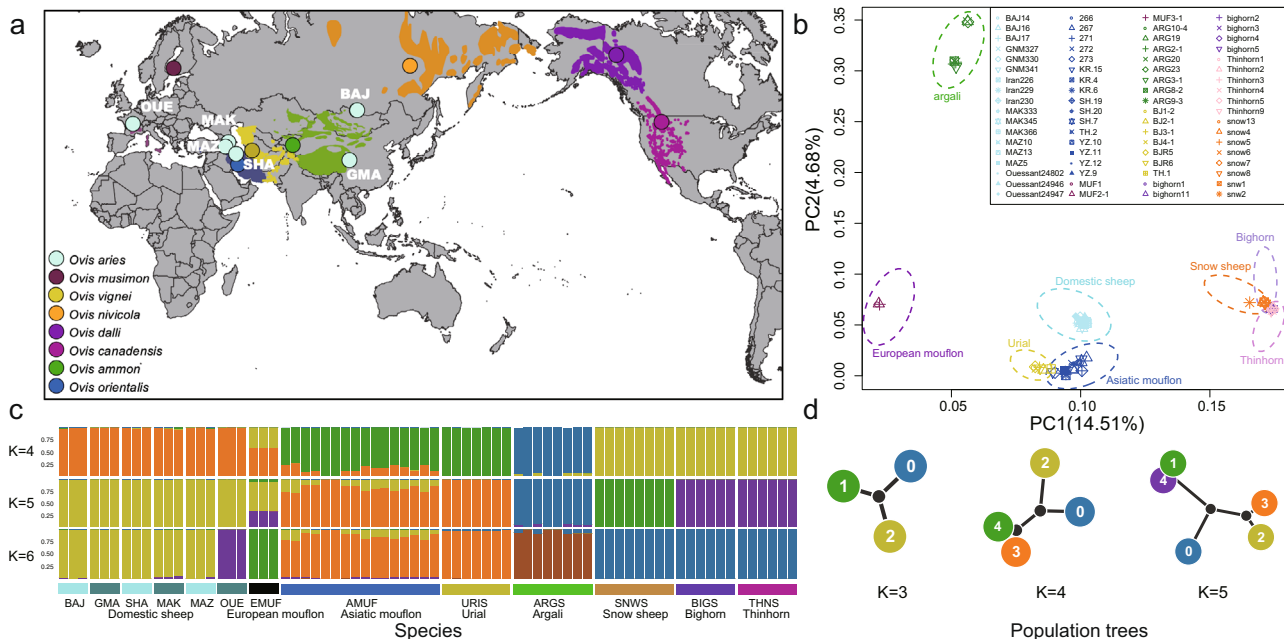


**Fig. 1 Geographic distribution and population structure of *Ovis* species.** **a** Geographic map of sample locations and wild sheep species distribution based on the IUCN Red list (<https://www.iucnredlist.org>). Here we adopted the classification of Nadler et al.<sup>66</sup> **b** Principal Component Analysis (PCA) of *Ovis* species. **c** Admixture plot using Ohana software for K from 4 to 6. **d** Population tree of each K indicates affinity of each ancestral component. Source data for **b**, **c** were presented in Supplementary Data 7.

**Table 1 Summary information of whole-genome variations identified in *Ovis* species.**

Sequence quality/variation type	Domestic sheep (n = 18)	Asiatic mouflon (n = 16)	European mouflon (n = 3)	Urjal (n = 7)	Argali (n = 8)	Snow sheep (n = 8)	Thinhorn sheep (n = 6)	Bighorn sheep (n = 6)
SNPs	31,535,487	53,618,832	13,360,034	30,125,980	25,160,871	22,845,295	23,185,374	23,069,044
INDELs	4,361,226	7,173,026	3,180,207	4,748,458	4,541,250	4,204,319	4,301,920	4,255,087
SVs	123,594	161,892	55,950	81,003	84,587	75,375	77,304	75,480
CNVs	74,672	92,366	37,250	56,216	52,236	48,705	48,794	48,527
Duplications	1814	2403	571	915	1185	1071	1122	1070
Deletions	72,858	89,963	36,679	55,301	51,051	47,634	47,672	47,457
Insertions	11,685	12,981	6517	8126	8867	7339	8954	8727
Inversions	746	1011	311	499	600	583	580	576
Translocations	36,491	55,534	11,872	16,162	22,884	18,748	18,976	17,650
Average depth (X)	19.25	27.11	18.89	19.77	17.78	17.8	19.43	18.88
Coverage rate (%)	97.2	98.22	97.03	97.1	96.79	96.54	96.65	96.62

“Methods” section), representing the eight *Ovis* species. Phylogenetic trees were then constructed from concatenated protein-coding regions (CDSs) of autosomes, the X chromosome, and the mitogenome of the assembled genomes, separately (Supplementary Fig. 5). These trees showed different phylogenetic patterns, but a consistent split between the three Pachycteriform species (i.e., bighorn, thinhorn, and snow sheep) and the others, being consistent with earlier genetic studies<sup>1,21</sup>. Together with the observation that the first fossil evidence of caprinae is in the Upper Vallesian in Spain<sup>21</sup>, these trees confirmed a Eurasian origin of the ovine species<sup>15,22</sup>.

We split the whole genome (one high-depth genome per species, see “Methods” section) into 2462 autosomal and 136 X-chromosomal 1 Mb non-overlapping windows of each species, and estimated Maximum likelihood (ML) trees for these windows. Three topologies (A, B, and C) were observed for 46.1%, 29.1%, and 17.8% of the autosomal trees, 33.8%, 50.0%, and 7.4% of the X chromosomal trees, respectively

(Supplementary Fig. 6). The main topologies A and B were also found using the maximum likelihood estimation on the concatenated CDSs (topology A, Fig. 2b) and using consensus methods of the Densitree on the non-overlapping fragments for autosomes (topology A, Fig. 2a) and X-chromosome (topologies B, Fig. 2a). We also estimated trees using high-depth individual autosomes and X-chromosome (Supplementary Fig. 5), which also support topologies A and B, respectively, while the individual mtDNA tree did not resemble any of the nuclear topologies.

The minor topologies (e.g., B and C for autosomes; and A and C for X-chromosome) may reflect local introgression between the species or incomplete lineage sorting (ILS) of ancestral phylogenies. The three phylogenies of all the 72 individuals using concatenated CDSs of autosomes (Fig. 2b and Supplementary Fig. 7a), X-chromosome and mitogenomes (Supplementary Fig. 7) showed seven major clades of individuals, with European mouflon sequences located among domestic sheep, compatible with the assumption that European mouflon is a domestic sheep

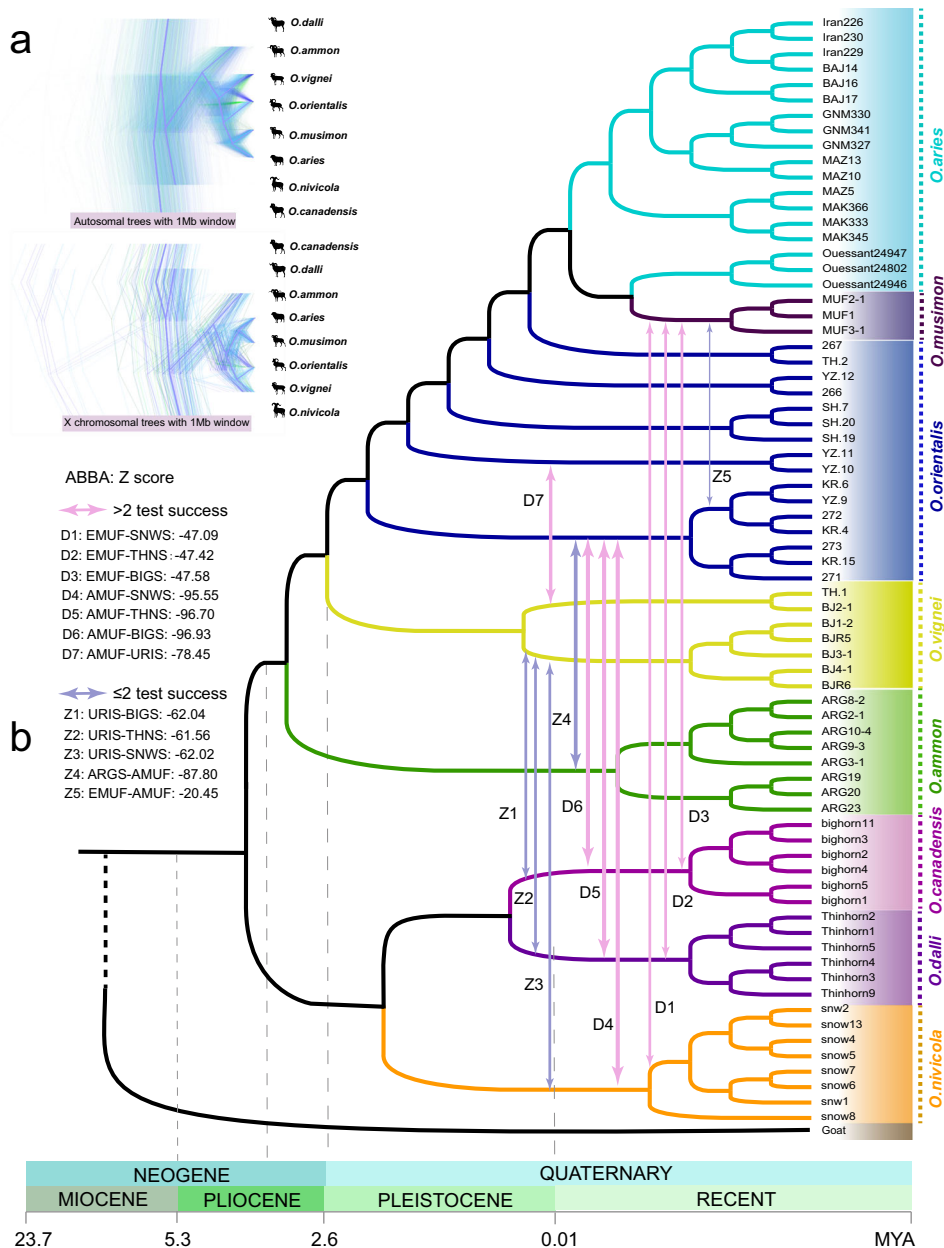


**Fig. 2 Phylogeny of *Ovis* genus.** **a** Prevalent discordance among segmental trees on autosomes and X chromosome, totaling 2598 1-Mb segments. The segmental trees were visualized by Densitree. Consensus tree topologies of each category are shown in purple. **b** Phylogenetic tree of the whole autosomal coding region (CDS) of the 72 individuals using RAXML. Arrows marked the introgression pairs and the corresponding Z-score based on the *D*-statistics, see Supplementary Data 4. Pink arrows indicate the admixed pairs which have been selected by three or more of the tests such as *D*-statistics, TreeMix, *f*-statistics, and admixture analysis, while purple arrows indicate the introgression pairs detected in two or less of the tests. Here, EMUF is European mouflon (*O. musimon*), AMUF is Asiatic mouflon (*O. orientalis*), URIS is urial (*O. vignei*), ARGS is argali (*O. ammon*), SNWS is snow sheep (*O. nivicola*), BIGS is bighorn sheep (*O. canadensis*), and THNS is thinhorn sheep (*O. dalli*). Source data for **a** were presented in Supplementary Data 7.

subspecies<sup>15</sup>. Also, European mouflon and domestic sheep show the same diploid number of chromosomes ( $2n = 54$ )<sup>1</sup>.

The phylogenetic trees (Supplementary Figs. 5, 7) and pairwise  $F_{ST}$  (Supplementary Fig. 8b) showed two clear clusters: the European mouflon and domestic sheep, and the Asiatic mouflon and the urial sheep. This is again compatible with the hypothesis that the European mouflon is a feral derivative of domestic sheep, but it also suggested that the Asiatic mouflons, sampled in Iran, have diverged considerably from the mouflon ancestors of both the early domestic hair sheep and the domestic wool sheep of more recent origin<sup>22</sup>.

A coalescent hidden Markov model (CoalHMM) based on autosomal sequences indicated a divergence time of domestic sheep and the three Pachyceriform species 0.244 to 0.270 Mya. Argali and urial were estimated to have diverged from domestic sheep ~0.124–0.150 Mya and ~0.077–0.092 Mya, respectively (Supplementary Figs. 9–11). The divergence time of the Asiatic mouflon and the urial was estimated to have occurred 0.073–0.083 Mya, which is earlier than the divergence between bighorn and thinhorn sheep (~0.036–0.052 Mya). An Isolation with Migration (IM) model<sup>23</sup>, which incorporates the impact of migration among species, gave a similar estimation with the Isolation (I) model<sup>23</sup>.



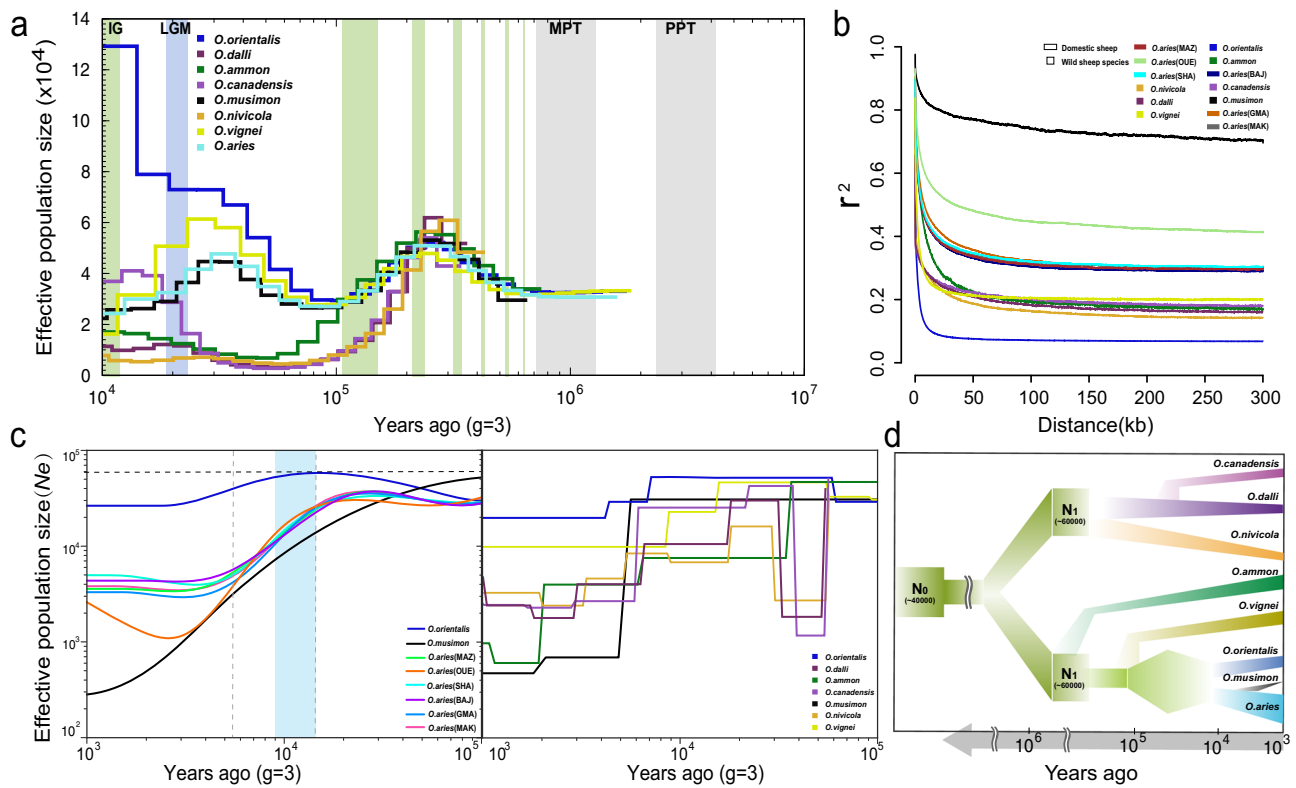


**Fig. 3 Demographic inference.** **a** Ancestral dynamic change of effective population size inferred by PSMC program for eight high-depth genomes. Colors of the lines indicated different species. Plots were scaled using a mutation rate of  $2.5 \times 10^{-8}$  per-site per generation and generation time (g) of 3. Light green shading indicates interglacials (IG) in the Pleistocene and Holocene, and light blue indicated as the Last Glacial Maximum (LGM) and gray shading indicates the mid-Pleistocene transition (MPT) and the Plio-Pleistocene transition (PPT). **b** LD decay analysis for seven wild species (marked as rectangles) and six domestic breeds (marked as squares). **c** Dynamic change of effective population size inferred by the SMC++ program for Asiatic and European mouflon and six domestic breeds (left panel) and seven wild species (right panel), the blue shading indicates the period of domestication and the gray vertical dashed line is the potential split time point of European and Asiatic mouflon. **d** Dynamic change of effective population size over time for all *Ovis* species. Source data for **b** were presented in Supplementary Data 7.

The relatively recent divergence of the European mouflon from domestic sheep 5550–5450 years BP (Supplementary Figs. 9–11) is concordant with the paleontological evidence of teeth and bone for a divergence of the Corsican mouflon and domestic sheep dated at 6000–5000 years BP<sup>24</sup>. Moreover, the coalHMM, IM, and I models, with a filtering threshold of <1000 years and >20,000 years for the split time<sup>14</sup>, showed a split time of 12,800–8800 years BP between domestic sheep and the Asiatic mouflon. This estimate is congruent with the estimated domestication time of sheep from the Asiatic mouflon around 9000–11,000 years BP, based on archeological data<sup>4,24</sup>, and also is in agreement with the time range 12,000–8000 years BP from the start of exploitation to the end of domestication<sup>25</sup>.

**Demographic history.** The pairwise sequentially Markovian coalescent (PSMC) model found a dramatic decline in population sizes of these species ~80–250 thousand years ago (kya) with a bottleneck for urial and Asiatic mouflon during 30,000–10,000 years BP (Fig. 3a), coinciding with the glacial periods. The subsequent increase in their population sizes can be ascribed to the prosperity of animal husbandry, agriculture, and sedentarism<sup>26</sup>. The SMC++ analysis showed a decline of all species 10,000–1000 years BP. In particular, we noted European mouflon has a more dramatic decline of effective population size ( $N_e$ ) than domestic sheep 6000–5000 years BP, which probably corresponds to the feralization of the European mouflon (Fig. 3c). The split between

domestic sheep and the Asiatic mouflon occurred during 15,000–9000 years BP. During this time period, the Asiatic mouflon showed an increased  $N_e$ , whereas domestic sheep experienced a severe bottleneck because of domestication.

**Genetic structure and differentiation.** PCA clusters individuals according to the recognized eight species. The cluster of argali showed significant within-species genetic divergence (Fig. 1b), which was also observed in the admixture pattern at high  $K$ -values (Supplementary Fig. 12). The Asiatic mouflon cluster was dispersed and overlapped partially with the urial cluster (Fig. 1c and Supplementary Fig. 12). The population tree was compatible with the inferred genetic clustering at  $K = 11$  (Supplementary Fig. 12a, b), in which each species was assigned to its own components. The admixture plot may suggest gene flow from argali (0.06–0.76%) and urial (1.4–15%) to Asiatic mouflon and possibly from wild relatives to domestic sheep, such as from European mouflon (5.4–5.7% of the genomes at  $K = 6$ ) to Ouessant sheep, an isolated island domestic breed (Supplementary Fig. 12). However, we noted that admixture proportions could not be interpreted as a direct evidence of admixture.

We observed higher levels of linkage disequilibrium (LD) in European mouflon and domestic sheep than in other species (Fig. 3b). This may be explained by a strong bottleneck during domestication. The Ouessant sheep<sup>27</sup> clearly had a higher LD than other domestic breeds, which was consistent with their low

genomic diversity (Fig. 3b and Supplementary Fig. 4). Likewise, the high LD in European mouflon could be explained by a small population size and possible bottleneck during its reintroduction from Corsica Island to the continental Europe<sup>15</sup>.

**Genomic introgression between wild species.** The ABBA–BABA analysis ( $D$ -statistic) was implemented using ANGSD-based on alignments, which suggested introgressions from bighorn, thinhorn, and snow sheep into their Eurasian relatives such as urial and Asiatic and European mouflons. (Supplementary Data 4). Statistical analyses based on variants using Admixtools (Supplementary Data 4), TreeMix (Supplementary Figs. 13 and 14), and  $f_d$ -statistics (Supplementary Fig. 15 and Supplementary Data 4) consistently showed significant introgression of snow, bighorn, and thinhorn sheep into urial, Asiatic and European mouflon. Bighorn and thinhorn sheep showed similar patterns of introgression as snow sheep in terms of several statistic indices, such as percentage (uriai: 6.23–6.33%, Asiatic mouflon: 3.63–3.7%, European mouflon: 1.43–1.47%), length (uriai: 152.68–155.1 Mb, Asiatic mouflon: 88.96–90.7 Mb, European mouflon: 35.08–35.96 Mb) and shared genes (uriai: 720–744, Asiatic mouflon: 449–468, European mouflon: 151–155) of introgression (Supplementary Fig. 15). We focus only on the snow sheep introgression. The introgression events into urial and Asiatic mouflon had a lot of overlaps in terms of genomic regions, while there was very minimal overlaps between Asiatic and European mouflon introgression segments (Supplementary Fig. 15 and Supplementary Data 4). Furthermore, admixture graph fitting based on  $f_d$ -statistics was carried out using the R package *admixturegraph* (Fig. 4), indicating a very close relationship between Pachyceriforms and European mouflon.

Signatures of introgression were detected in candidate regions overlapping 892 genes from snow sheep to urial sheep. These genes were significantly (false discovery rate, FDR of 0.05 by the method of Benjamini–Hochberg<sup>28</sup>) enriched in nerve conduction, energy metabolism, membrane signal transduction, bile secretion, drug addiction, and motor activity using DAVID annotation tools. From snow sheep to Asiatic mouflon or European mouflon, we found candidate introgression regions covering 497 and 179 genes, respectively (Supplementary Fig. 15a). In European mouflon, the introgressed genes were enriched in nerve regulation, locomotory behavior, cardiac disease, insulin secretion, serotonin metabolic process, and calcium signaling pathways, while in Asiatic mouflon the genes were enriched in walking behavior, regulation of cell differentiation, ovarian steroidogenesis, and platelet activation. Noteworthy, we observed three shared GO terms for the genes involved in the inter-species introgression events, such as motor, iron channel activity, and dendrite development. (Supplementary Data 4).

Among the three sets of introgressed genes between wild species, we observed 12 shared genes (*CYP2J*, *PRUNE2*, *ZNF385B*, *IMMP2L*, *GRIK2*, *HS6ST3*, *USH2A*, *LOC101111335*, *TMEM132D*, *PAG11*, *PAG3*, and *CTNNA3*), which have functions associated with reproduction and production traits such as follicular development (*CYP2J*, *IMMP2L*), prolificacy (*GRIK2*), growth (*HS6ST3*), wool and body weight (*TMEM132D*)<sup>29–34</sup>, and nervous response such as hearing ability evolution (*USH2A*) and nerve development (*PRUNE2*)<sup>35,36</sup>. In particular, shared signatures of introgression were observed in the PAG gene family, which is involved in pregnancy detection and placental viability evaluation<sup>37</sup>. Moreover, these genes were significantly enriched in a GO term (GO:0004190), which consists of pregnancy-associated glycoproteins (*PAG3* and *PAG11*) related to aspartic-type endopeptidase activity. We also observed one marginally significantly enriched KEGG pathway of protein digestion and

absorption (oas04974) including the two genes from the PAG gene family.

**Dating the introgression from wild relatives into Asiatic mouflon.** In addition to the introgression from snow sheep into Asiatic mouflon (Fig. 5a–d) mentioned above,  $D$ -statistics,  $f_3$ -statistics, and TreeMix analysis also detected signatures of introgression from argali into Asiatic mouflon (Supplementary Data 4 and Supplementary Figs. 13 and 15a). Across-genome  $f_d$ -values detect 670 and 734 segments introgressed from snow sheep and argali, respectively, corresponding to a genomic coverage of 3.68% and 3.98%, containing 497 and 540 genes. (Supplementary Data 4). The program DATES yielded time estimates for the snow sheep and argali introgression events of 3481 and 2493 generations ago, respectively. Similar estimates were obtained with Ancestry\_hmm: 3096 and 2545 generations ago (Supplementary Fig. 16). With a generation time of 4 years for Asiatic mouflon, both methods indicated that the introgression from snow sheep, as well as from bighorn and thinhorn sheep, occurred before the domestication (13,924–11,580 years BP). In contrast, the introgression from argali to Asiatic mouflon at 9,972–10,180 years BP coincides with the domestication process. Because introgression of argali into domestic sheep is confined to sympatric populations<sup>16,38</sup>, we believe that the gene flow between argali and Asiatic mouflon did not take place until after the domestication process, resulting in the first domestic sheep lacking gene flow from argali. The gene flow from argali was probably also absent in the mouflon population ancestral to domestic sheep. GO categories and KEGG pathway of snow sheep and argali introgression into Asiatic mouflon were reported in Supplementary Data 4.

**Selection signatures in domestic sheep.** To detect selection signatures in domestic sheep, we used pairwise differences  $\pi$  ratio ( $\pi_w/\pi_d$ ) >2.36 and  $F_{ST}$  between domestic sheep and Asiatic mouflon. We selected the overlap of the top 10% outliers in both methods, identifying 340 windows as candidate regions for selection. These regions contained a set of 131 selective functional genes (Supplementary Data 5 and Fig. 5e, f) which were significantly ( $P < 0.05$ ) enriched in GO terms involved in the activation of the innate immune response, positive regulation of defense response to virus by host, ectoderm development, membrane transport and enzyme activity (Fig. 5g). Of the 131 genes, 62 (47%) overlapped with domestication-related genes in previous studies, and were defined as the candidate domestication genes in sheep (Supplementary Data 5). Remarkably, of these candidate domestication genes 11 and 13 (15,365 genes on autosomes, significantly overlapped between two gene lists with Fisher's exact test,  $P < 0.01$ ) have been introgressed into Asiatic mouflon from snow sheep and argali (Fig. 5e, f). These genes were functionally involved in immune response (*HERC3* and *NFYA*), visual evolution (e.g., *RNF24*), resistance to the virus (e.g., *SIN3A*)<sup>39–42</sup>, production and reproductive traits [e.g., milk and protein yield (*SH3GL3* and *PAPPA2*)], fecundity (*DNAJB14* and *FSIP2*), body measurement (*SIRT3* and *SH3GL3*), tail type (*HAO1*), regulation of osteogenesis (*GTF2I*), skeletal muscle development (*ZNF777*) and lumbar vertebrae number traits (*NR6A1*)<sup>43–52</sup>, and environmental adaptation [e.g., superior heat tolerance (*PPP2R5E*, *GTF2IRD1*, and *DNAJB14*)]<sup>53–55</sup>.

Of special interest was the introgressed genomic region chr3: 10,980,301–11,211,252, which contains gene *NR6A1* and had the highest (OUE, AMUF; SNWS, goat)  $f_d$ -value (Fig. 6). We also computed the mean pairwise sequence divergence ( $d_{xy}$ ) of snow sheep and Asiatic mouflon or Ouessant sheep. This region also had a reduced mean pairwise sequence divergences ( $d_{xy}$ ) of snow sheep and Asiatic mouflon, a high  $d_{xy}$  of snow and Ouessant

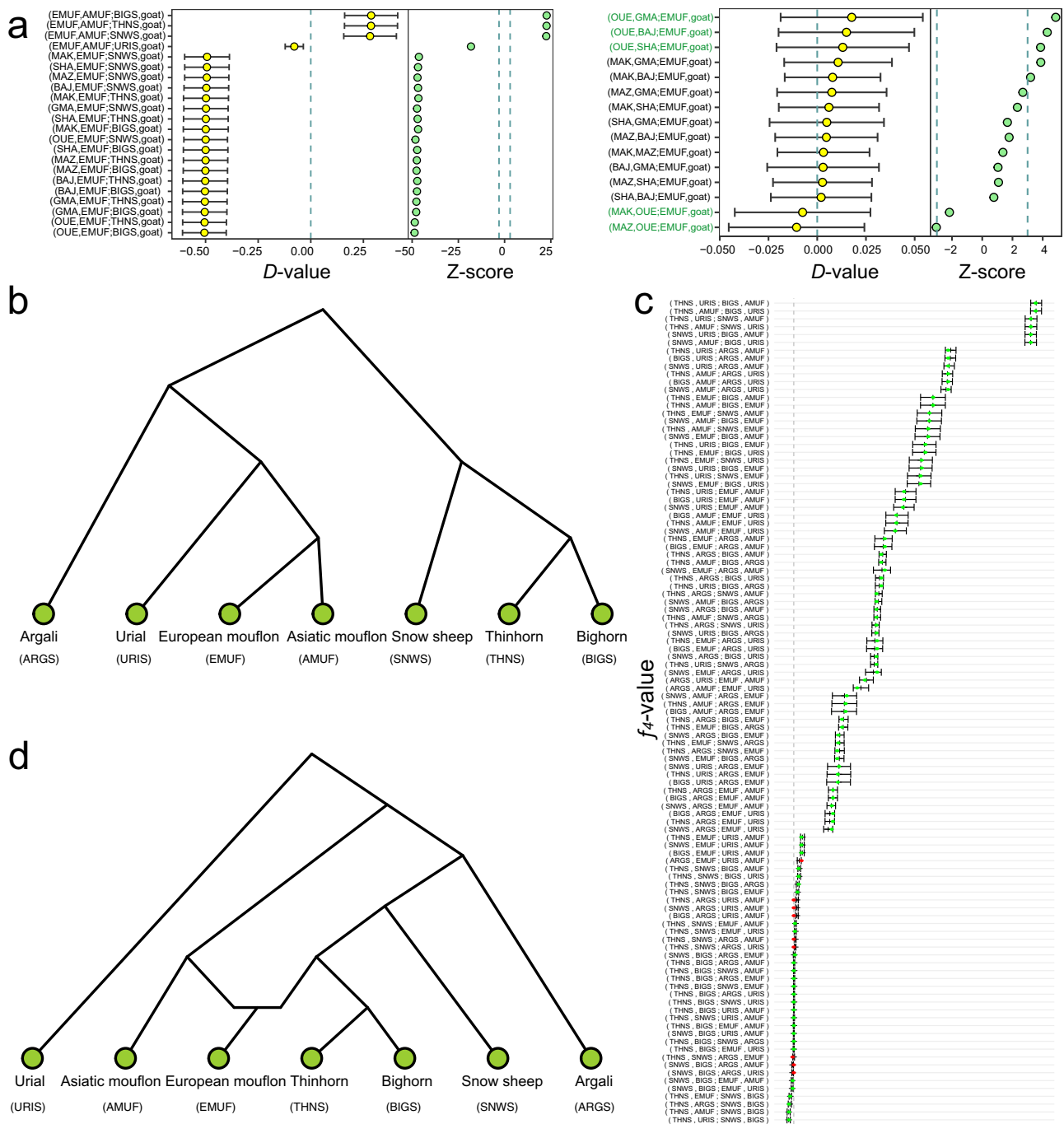


**Fig. 4** Admixture graph fitting for introgression from the Pachyceriforms into European mouflon. **a**  $D$ -statistics of European mouflon (EMUF) with the Pachyceriforms [snow sheep (SNWS), bighorn (BIGS), and thinhorn sheep (THNS)]. **b** Prior phylogeny of wild species in *Ovis* genus. **c** Goodness of fit of  $f_4$ -statistics. **d** Admixture graph. Source data for **a**, **c** were presented in Supplementary Data 4.

sheep, and a low differentiation ( $F_{ST}$ ) of Asiatic mouflon and snow sheep, all indicating introgression of snow sheep into Asiatic mouflon (Fig. 6a–c).

For the 11 genes introgressed from snow sheep into Asiatic mouflon, haplotype comparisons for the SNPs in the introgressive regions from argali, snow sheep, Asiatic mouflon, and domestic sheep were shown in Fig. 6d, e. Notably, we found that the haplotype patterns of Asiatic mouflon strongly resembled those of snow sheep and argali, but differed strikingly from the patterns observed in the domestic sheep (Fig. 6d, e). Haplotype patterns showed most of the introgressive haplotypes of genes (e.g., *NR6A1*, *FSIP2*, *ZNF777*, *RNF24*, and *PPP2R5E*) have not been

selected and fixed in domestic sheep (Fig. 6d, e). Since most of the domestication-related genes are associated with production traits, this scenario could be explained by that introgressions associated with adaptation rather than production traits have been mostly selected in the genetic improvement stage after domestication<sup>38</sup>.

**Common introgressions between wild and domestic sheep.**

In the introgression test ( $D$ -statistics and TreeMix analysis) between wild and domestic sheep, we found significant signatures of gene flow from (i) European mouflon into Ouessant sheep (OUE), (ii) urial and Asiatic mouflon into Shal (SHA), and (iii) argali into



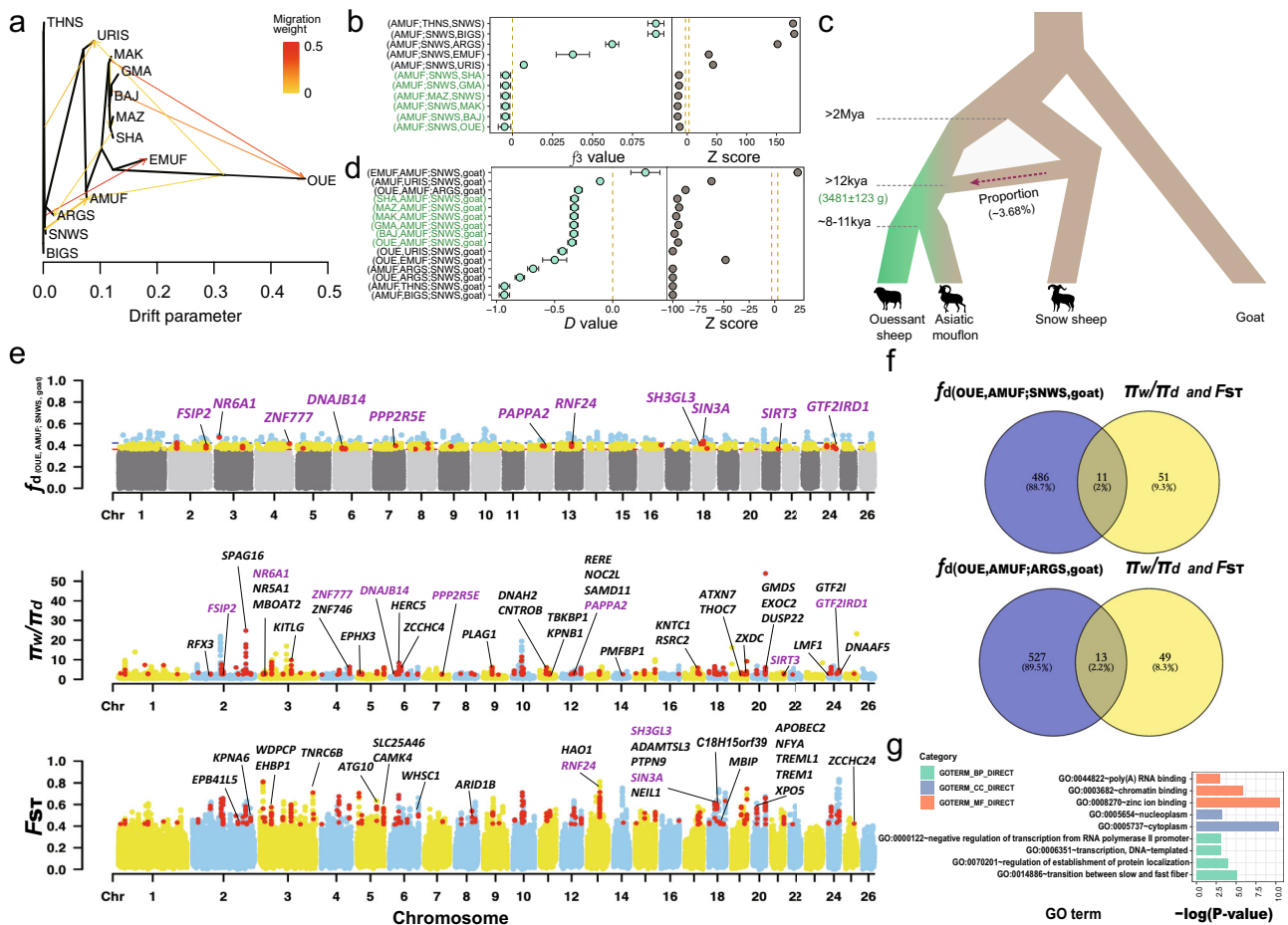


**Fig. 5** Local inference and annotation of introgression signals from snow sheep to Asiatic mouflon. **a** Treemix analysis when  $m = 9$ . **b, d**  $f_3$ -statistics and  $D$ -statistics of Asiatic mouflon (AMUF) with snow sheep (SNWS) pairs. Double dashed line marked as the range of threshold from -3 to 3. **c** Demographic diagram of admixture from snow sheep (*O. nivicola*) to Asiatic mouflon (*O. orientalis*). **e** Introgressed regions identified in the Asiatic mouflon genome. A modified  $f$ -statistic ( $f_d$ ) for (OUE,AMUF;SNWS,goat),  $\pi$  ratio ( $\pi_w/\pi_d$ , i.e.,  $\pi$  of Asiatic mouflon/and  $\pi$  of all the domestic sheep) and  $F_{ST}$  between Asiatic mouflon and all the domestic sheep for 100-kb windows with 20-kb steps is plotted along the chromosomes. Each dot represents a 100-kb window. For  $f$ -statistic, green and blue dots above the red horizontal line correspond to the FDR 5% and FDR 1% significance level thresholds, respectively. The regions containing genes among three indexes ( $f_d$ ,  $\pi$  ratio, and  $F_{ST}$ ) are plotted in red dots, and 62 verified candidate domestication genes are marked in the plot. Overlapped genes ( $n = 11$ ) with  $f$ -statistic are marked in purple. **f** Venn diagram of overlapping genes ( $n = 11$  for snow sheep and  $n = 13$  for argali) between introgressed genes ( $n = 497$  for snow sheep and  $n = 540$  for argali) and candidate domestication genes ( $n = 62$ ). **g** GO enrichment for 62 overlapped domestication genes with the previous studies. Source data **d-g** were presented in Supplementary Data 4 and Supplementary Data 5.

Tibetan sheep (GMA) (Fig. 4a, Supplementary Data 4, and Supplementary Figs. 13, 17). We detected 154 genes located in the introgressed tracts from European mouflon to Ouessant sheep. These genes were significantly enriched in the GO terms and KEGG pathways of nerve conduction and development (e.g., GO:0007269, GO:0098793, GO:0043065, GO:0090129, GO:0051965, and oas04360), cell adhesion (GO:0007156), intracellular signal transduction (GO:0035556 and oas04024) and walking behavior (GO:0007628) (Supplementary Data 4).

We identified regions containing 516 and 430 introgressed genes from the Asiatic mouflon or urial into Shal sheep, 251 of these were shared between the two species (Supplementary Data 4 and Supplementary Fig. 17). All these genes were significantly ( $P < 0.05$ ) enriched in the GO terms with functions in tissue and organ development, reproduction, and morphological change. In these tests of introgression from wild sheep to their sympatric domestic relatives, shared signals were detected in 10 functional genes (e.g., *CCDC67*, *FAT3*, *PCDH15*, and *NEURL1*). These 10 common genes have functions associated with arid environment

adaptation (*FAT3*)<sup>56</sup>, immune response (*PCDH15*)<sup>57</sup>, nervous response (*NEURL1*)<sup>58</sup>, and disease susceptibility like noise-induced hearing loss (*PCDH15*)<sup>59</sup>. Moreover, the genes introgressed from argali to Tibetan sheep were significantly enriched in GO terms in olfactory bulb development (e.g., *AGTPBP1*, *CRTAC1*, and *RPGRIP1L*) and synaptic transmission (e.g., *GRIK2*, *PARK2*, and *SHC3*) (Supplementary Data 4). Notably, two introgressed genes from Asiatic mouflon to Shal sheep (i.e., *REFX3* and *DNAJB14*) and one introgressed gene from argali to Tibetan sheep (i.e., *CAMK4*) were identified to be under domestication (Supplementary Data 4 and Supplementary Data 5).

**Probability of incomplete lineage sorting (ILS).** We estimated the probability of incomplete lineage sorting (ILS) for the introgressed tracts identified from argali and snow sheep into the Asiatic mouflon. The expected length of a shared ancestral tract (see “Methods” section) is  $L_{\text{snow}} = 1/(1.5 \times 10^{-8} \times (2.3 \times 10^6)/4) = 115.94$  bp,  $L_{\text{argali}} = 1/(1.5 \times 10^{-8} \times (1.72 \times 10^6)/4) = 155.04$  bp and

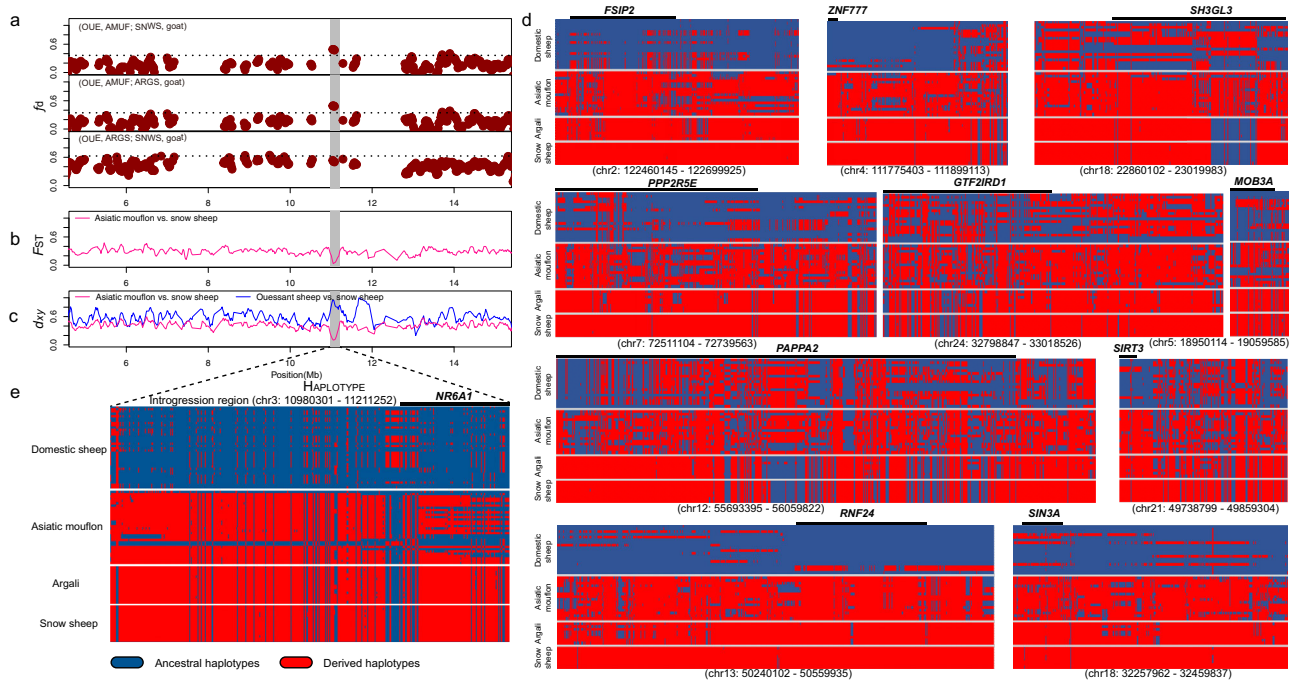


**Fig. 6** Local inference of genomic region at genes introgressed from snow sheep (SNWS) into Asiatic mouflon (AMUF). **a**  $f_i$  statistics ( $f_i$ ) based on (OUE, AMUF; SNWS, goat) comparison with (OUE, AMUF; ARG, goat) and (OUE, ARG; SNWS, goat) calculated for 100-kb windows with 20-kp steps across the genome for Asiatic mouflon. Each dot represented a 100-kb window, and the dashed line indicated the significance threshold ( $P < 0.05$ ). **b** Population differentiation ( $F_{ST}$ ) around the introgressive genomic region between recipient (Asiatic mouflon) and donor (snow sheep). **c** Mean pairwise sequence divergence ( $d_{xy}$ ) of the introgression region between snow sheep and either Asiatic mouflon or Ouessant (OUE) domestic sheep population. **d, e** Haplotype patterns among all the domestic sheep, Asiatic mouflon, argali, and snow sheep for the 11 genomic regions. Genes within the introgressed segments were marked above haplotypes.

the probability of a length of at least 96,410 bp and 98,037 bp (i.e., the observed introgressed regions containing the domestication-related genes were 96,410–319,834 bp and 98,037–639,187 bp) is negligible ( $1 - \text{GammaCDF}(96,410, \text{shape} = 2, \text{rate} = 1/L) = 0$ ) (Supplementary Data 6). Similarly, the probability of common introgressed tracts appearing due to ILS detected from snow sheep to European mouflon and urial, and urial to domestic sheep approach zero, and Asiatic mouflon to domestic sheep is less than 0.05. However, the possibilities of ILSs for the common tracts introgressed from European mouflon to domestic sheep was relatively high (Supplementary Data 6). Thus, the inter-species common introgressions detected above were unlikely due to ILS except for European mouflon.

## Discussion

In this study, we generated a genomic data set of high-depth whole-genome sequences of domestic sheep and their wild relatives, including the wild ancestor of sheep (Asiatic mouflon), and the vulnerable (e.g., urial) and near-threatened species (e.g., argali) according to the International Union for Conservation of Nature (IUCN) Red List. Our genomic data included different types of molecular markers such as SNPs, SVs, CNVs, and INDELs, providing an important resource for the genetic improvement of sheep, as well as for ecological and evolutionary studies of the wild species.

This is the first comprehensive and in-depth investigation on phylogeny and introgressions among the whole *Ovis* genus. Different from the previous studies<sup>1,60</sup>, multiple up-to-date analyses were applied to cross-validate the obtained results. For example, to better understand the trajectories of connections between admixture events and phylogenetic relationships across the whole genome, we used sliding window-based and fitting-based

methods to construct the consensus trees. Additionally, we implemented the introgression tests based on several statistical approaches such as  $D$ -statistics,  $f_i$ -statistics, TreeMix, and admixture analyses. Further, we verified the introgression events (including introgression sources and time) using the admixture graph fitting method and dated the introgression time using both model-based and LD decay-based methods. All the analyses showed accordant results.

We verified our SNPs based on both statistical and experimental methods, securing the data set for the subsequent analysis. By comparing with other species, we found on average 17.61 million SNPs per individual (9–21 SNPs/kb among the *Ovis* species), which is less than that in goat (53–54 SNPs/kb)<sup>61</sup>, but higher than that in swine (1 SNP per 10.3 kb)<sup>62</sup>.

Within the *Ovis* species, a relatively low diversity and effective population size (4000–10,000) in the Pachyceriforms may be ascribed to long-term geographic and genetic isolation<sup>1,21</sup> and is relevant for its conservation. The much less genetic diversity observed in Pachyceriforms than that in Moufloniforms could be due to (i) the common ancestor of Pachyceriforms should have migrated out from Eurasia, the distribution region of Moufloniforms, with genetic drift and differentiation between each other; and (ii) the genome of domestic sheep has been used as the reference for SNP mapping, while domestic sheep is phylogenetically further from Pachyceriforms than Moufloniforms. We observed the highest diversity in Asiatic mouflon ( $\pi = 0.0044$ ), which was much higher than in domestic sheep ( $\pi = 0.0032$ ). This has been observed previously<sup>63</sup> and can be explained by the domestication bottleneck<sup>64</sup>. Our results also showed lower diversity estimates than previous investigations using whole-genome BeadChip SNPs and mtDNA variation<sup>63,65</sup>. Higher estimates from the BeadChip could be explained by the ascertainment bias in the chip design.

Previous molecular evidence for taxonomic classification has so far mostly been based on mtDNA sequences<sup>1,60,66</sup>. However, pervasive and frequent autosomal introgressions<sup>14,16</sup> probably account for the lower estimates of the coalescence time compared with those from mtDNA sequences<sup>1,60</sup>. In particular, the evidence from SMC++, CoalHMM statistics, phylogenetic trees, admixture analysis, and mean population differentiation ( $F_{ST}$ ) index indicated a more recent divergence of European mouflon and domestic sheep (~5000 years BP), than estimated on the basis of mtDNA sequences (~21,000 years BP)<sup>67</sup>. The recent divergence of European mouflon from domestic sheep was also supported by archeological data<sup>24</sup>. Our evidence confirmed that European mouflon emerged as feral domestic sheep when the earliest wave of domestic hair sheep, was displaced by a second wave of wool sheep<sup>15,68,69</sup>.

Also, we obtained a more recent split time between argali and domestic sheep (~0.12–0.15 Mya) than earlier estimates. The earlier divergence time was based on orthologous genes using PAML and the node was calibrated using four fossil records such as the divergence of the opossum and human (124.6–134.8 million years ago [Mya]), human and taurine cattle (95.3–113 Mya), taurine cattle and pig (48.3–53.5 Mya), and taurine cattle and goat (18.3–28.5 Mya)<sup>70</sup>. Also, different estimates of  $1.72 \pm 0.36$  Mya and ~2.93 Mya were obtained from mitochondrial sequence variations<sup>1,60</sup> using the five fossil calibration time of 18.3–28.5 Ma between Bovinae and Caprinae, 52–58 Ma between Cetacea and hippopotamus, 434.1 Ma between baleen and toothed whales, 42.8–63.8 Ma between Caniformia and Feliformia, and 62.3–71.2 Ma between Carnivora and Perissodactyla. This difference could be due to different mutation rates of the whole genomes and mtDNA sequences, and different calibration time points have been used in different studies. Additionally, we used two model of coalHMM (Isolation with migration and Isolation model) with full consideration of migration after speciation, and the estimates have always been lower than those estimated by mtDNA sequences and protein-coding genes<sup>71</sup>. Besides these, the more recent divergence time estimated here could be attributed to the extensive genomic introgressions between the sequenced genomes of the two species.

Remarkably, the Admixture and Treemix patterns, as well as  $D$ -statistics and  $f_d$ -statistics consistently showed introgression of the Pachyceriforms (snow sheep, bighorn and thinhorn sheep) into European mouflon. The Pachyceriforms also introgressed Asiatic mouflon, but this was a more recent event and involved a different set of genomic segments (Supplementary Fig. 15). The introgression percentage as inferred by  $f_d$ -statistics were 1.47%, 1.45%, and 1.43% from bighorn, thinhorn, and snow sheep to European mouflon, while higher introgression percentages of 3.7%, 3.63%, and 3.68% were from bighorn, thinhorn, and snow sheep to Asiatic mouflon. This indicated that the wild ancestors of the European mouflon, and consequently also the first hair sheep domesticated, descended from a population that differs from the Asiatic mouflons in this study, which were sampled in Iran. In contrast, the Iranian Asiatic mouflons are phylogenetically diverse and close to urial, which is in line with the mtDNA (Supplementary Fig. 7) and Y-chromosomal phylogeny<sup>19</sup>. As the range of snow sheep and their American relatives did not extend to Europe, our results suggested that European mouflons might have partially descended from a now-extinct sheep in Europe and arose through hybridization events between this species and feral domesticated sheep (Fig. 4 and Supplementary Fig. 7). Some wild sheep species live in extreme environments, such as snow sheep in the extreme cold arctic regions, and argali on the cold Qinghai-Tibetan Plateau and the Pamir Highland. Thus, our data may be relevant for environmental adaptation. However, it's challenging to confirm the ancient introgression trajectories based on modern

samples, ancient samples of *Ovis* species are necessary to answer this question.

Recently, there has been a strong interest in inter-species introgression, particularly from wild relatives to domestic animals such as pig, goat, and sheep<sup>9,10,13,15</sup>. For example, an earlier study has shown adaptive introgression and selection on domestic genes in goat<sup>72</sup>. In particular, *MUC6* was found to be introgressed from a West Caucasian tur-like species into modern goat during domestication, and was nearly fixed in domestic goat with the function of pathogen resistance<sup>72</sup>. In the *Ovis* genus, hybridization among species has been documented in the previous field and molecular studies<sup>6,9,66</sup>. However, adaptive introgression from distantly related wild species into the wild ancestors of domestic animals or into domestic animals has rarely been investigated<sup>72,73</sup>. Genomic signature of adaptive introgression from European mouflon into domestic sheep has been previously reported<sup>15</sup>. An earlier whole-genome SNP analysis suggested that historical introgression from wild relatives was associated with climatic adaptation and that introgressed alleles in *PADI2* have contributed to resistance to pneumonia in sheep<sup>38</sup>.

A strong signature of adaptive introgression from argali into Tibetan sheep was detected, and the introgressive genes involved in hypoxia and ultraviolet signaling pathways (e.g., *HBB* and *MITF*) and associated with morphological traits such as horn size and shape (e.g., *RXFP2*). The introgressed genes were related to adaptation to the extreme environment in the Qinghai-Tibetan Plateau<sup>16</sup>. We also identified other genes in Tibetan sheep introgressed from argali, associated with disease resistance to pathogens (e.g., *ACTN4*), and with olfactory development (e.g., *AGTPBP1*), and locomotion (e.g., *OXR1*), possibly related to adaptation to the semi-wild grazing and anoxic environments in plateau. Furthermore, we found patterns compatible with adaptive introgression from the Pachyceriform sheep and argali into urial, Asiatic mouflon, and European mouflon. However, it is challenging to validate the function of these genes in vivo or in vitro in the wild animals.

We detected adaptive introgression from various wild species into Asiatic mouflon, covering several domestication-related genes. Inspection of these domestication-related genes (e.g., *KITLG*, *CAMK4*, *NR6A1*, *RNF24*, *MBIP*, *SH3GL3*, *GMDS*, *EXOC2*, and *GTF2I*) indicated their functions associated with important morphological, physiological, and production traits such as litter size and mammary cycle<sup>74,75</sup>, early body weight (e.g., *PLAG1*<sup>76</sup>), regulation of follicular development (e.g., *NR5A1*<sup>77</sup>) in sheep. Theoretically, particular functions of these domestication-related candidate genes indicated relevant traits have been the targets under intensive selective pressure during the domestication process, which eventually led to emergence of the typical morphological, production, physiological, and behavioral differences between domestic sheep and their wild ancestors<sup>78</sup>. In practice, the highly differentiated non-synonymous mutations in coding regions of the genes should be functionally important and could be integrated in marker-associated selection and genomic selection for related traits in future genetic improvement of domestic sheep<sup>17</sup>.

In conclusion, we estimated the phylogenetic relationships of the sheep species on the basis of high-depth whole-genome sequences. Our results suggested a feral origin of domestic sheep for European mouflon around 6000–5000 years BP and a genetic overlap of urial and the Iranian Asiatic mouflon. We found extensive introgression events among the *Ovis* species, which partially overlapped with regions under selection in domestic sheep. Our results provide important insights into changes in the genome landscapes of domestic sheep and their wild ancestor occurring during and after domestication.



## Methods

**Samples and DNA extraction.** Seventy-two whole-genome sequences of 6 domestic breeds ( $n = 18$ ) and wild species ( $n = 54$ ) of the genus *Ovis* were included in this study (Supplementary Data 1). Here we followed the classification of Nadler et al.<sup>66</sup> due to the greatest taxonomy number. The classification was based on morphological traits and chromosome diploid number. These domestic breeds were selected from sheep, which have shown genomic introgressions from sympatric wild relatives.<sup>15,16,38</sup> Thirty-four whole-genome sequences were sequenced in this study and 38 were from our previous studies<sup>17,19</sup>. The 34 genomes generated here consisted of 5 domestic sheep from 3 populations, including Tibetan sheep (GMA, Maqu county, Gansu), Mazekh sheep (MAZ) in Azerbaijan and Makui sheep (MAK) in Iran, and 29 wild sheep from 6 species, including *O. musimon* ( $n = 3$ ), *O. orientalis* ( $n = 1$ ), *O. vignei* ( $n = 5$ ), *O. nivicola* ( $n = 8$ ), *O. dalli* ( $n = 6$ ) and *O. canadensis* ( $n = 6$ ), all of which were understudied in previous studies. The 38 public genomes comprised 13 domestic sheep (3 French Ouessant (OUE) sheep sampled in the Netherlands, 3 Baidarak sheep (BAJ) from Russia, 3 Shal sheep (SHA) from Iran, 1 Tibetan sheep, 2 Makui sheep and 1 Mazekh sheep), and 25 wild sheep genomes from 3 species (*O. orientalis*,  $n = 15$ ; *O. ammon*,  $n = 8$  and *O. vignei*,  $n = 2$ ; Supplementary Data 1). Historical information, geographic distribution, and morphological traits such as body size, horn morphology, color, and pattern of the coat have been used in the definition of species<sup>79</sup> and types and varieties of hair and wool sheep<sup>27</sup>. Genomic DNA was extracted from the blood or tissue samples using the standard methods of proteinase K solution and phenol-chloroform extraction<sup>80</sup>. DNA samples with a clear band in sepharose gel, an OD<sub>260</sub>/OD<sub>280</sub> ratio between 1.7 and 2.0, and a concentration at least 20 ng/μL were used for the library construction.

**DNA sequencing and read filtering.** Whole-genome sequencing was performed using the Illumina HiSeq Xten. At least 1.5 μg of genomic DNA from each sample was sheared into 180–500 bp small fragments using the Covaris S220 instrument (Covaris, Woburn, MA, USA) and used for Illumina library preparation. Sequencing libraries were constructed using the Truseq Nano DNA HT Sample preparation Kit (Illumina Inc., San Diego, CA, USA) following the manufacturer's instructions. In brief, DNA fragments were end-repaired, A-tailed, ligated to paired-end adapter, and the fragments with ~350 bp insert length were selected for amplification by 8–12 cycles of PCR using the Platinum Pfx Taq Polymerase Kit (Invitrogen, Carlsbad, CA, USA). PCR products were purified with the AMPure XP system (Beckman Coulter, Brea, CA, USA), and libraries were analyzed for the size distribution by the Agilent 2100 Bioanalyzer (Agilent Technologies, Palo Alto, CA, USA) and quantified in real-time PCR. The constructed libraries were sequenced on the Illumina HiSeq X Ten platform (Illumina Inc.) and paired-end 150 bp reads were generated.

All the newly generated and retrieved whole genomes ( $n = 72$ ) were included in the following analyses. On average, 95.83% of the sheep reference genome was covered by the depth of  $\geq 4\times$ , 90.11% was covered by  $\geq 10\times$ , and 46.68% was covered by  $\geq 20\times$ . To obtain reliable reads, we removed the raw paired-reads that meet any of the following three criteria: (i) unidentified nucleotides (N-content)  $\geq 10\%$ ; (ii) reads pair with adapters; and (iii)  $> 50\%$  of the read bases with a phred quality (Q) score  $< 5$ .

**Reads mapping, variant detection, quality control, and annotation.** Clean reads were mapped to the sheep reference genome OARv4.0 (GCA\_000298735.2) using the BWA v0.7.17 MEM module<sup>81</sup> with the parameters `bwa -k 32 -M -R`. Duplicates were removed using Picard MarkDuplicates and sorted using Picard SortSam (<https://broadinstitute.github.io/picard/>). To obtain reliable alignments, the reads meeting any of the following three criteria were filtered: (i) unmapped reads; (ii) reads not mapped properly according to the aligner used above; and (iii) the reads with RMS (root mean square) mapping quality  $< 20$ . Base-quality score recalibration (BQSR) with ApplyBQSR module (default parameters) was used to detect the systematic errors during the sequencing process.

Variant discovery was carried out using the Genome Analysis Toolkit (GATK-v4.0.4.0) best practices pipeline, followed by a joint genotyping method on all samples in the cohort<sup>82</sup>. In summary, we firstly called the variants based on each sample using Haplotypecaller module in GVCF mode with the parameter-genotyping-mode DISCOVERY-min-base-quality-score 20-output-mode EMIT\_ALL\_SITES-emit-ref-confidence GVCF. Then, we implemented the joint genotyping procedure by consolidating all the GVCFs with the GenotypeGVCFs module. Furthermore, we combined all the variants using CombineGVCFs. Variant sites were identified for each of the eight species, separately. Within each species, the following successive filtering processes were applied for the variant site and genotype quality control: first, raw SNPs were hard filtered using the VariantFiltration module with the strict parameters-filter-expression QUAL  $< 30.0$  | QD  $< 2.0$  | MQ  $< 40.0$  | FS  $> 60.0$  | SOR  $> 3.0$  | HaplotypeScore  $> 13.0$  | MQRankSum  $< -12.5$  | ReadPosRankSum  $< -8.0$  in each species, separately. We then merged all the 8 variant datasets from eight species using the bcftools merge function after the bcftools index. In addition, PLINK v1.9<sup>83</sup> was used to filter SNPs that meet any of the following criteria: (i) proportion of missing genotypes among all the individuals over 10% (geno 0.1); (ii) SNPs with minor allele frequency (MAF) higher than 0.05 (maf 0.05); (iii) SNPs showing an excess of heterozygosity (-hwe 0.001); and (iv) non-biallelic sites. This yielded a high-quality set of variants including 6,558,545 SNPs obtained for the genomic introgression

and diversity analyses. For analyzing population genetic structure, we excluded SNPs in LD with  $r^2 \geq 0.2$  (-indep-pairwise 50 5 0.2). All the SNPs were annotated using the ANNOVAR v.2013-06-21 software<sup>84</sup> and phased using Shapeit v4.1.3<sup>85</sup>.

**SV detection and annotation.** To identify reliable structural variants (SVs), we detected the SVs by implementing four independent calling pipelines. First, SVs were detected based on the filtered and sorted BAM file using novoBreak v.1.1.3<sup>86</sup>, which detects deletions (DEL), inversions (INV), tandem duplications (DUP), and inter-chromosomal translocations (TRA). Second, SVs were identified using configManta.py in manta v.1.6.0<sup>87</sup>. Manta reports SVs as deletions (DEL), inversions (INV), tandem duplications (DUP), insertions (INS), and inter-chromosomal translocations (TRA). Third, SVs were detected using GRIDSS v2.6.2<sup>88</sup>. SV files in VCF format were then annotated using a custom R script (<https://github.com/PapenfussLab/gridss/blob/master/example/simple-event-annotation.R>). GRIDSS generates the same variant types of SVs as those by manta. These three pipelines utilized the same input of 72 BAM files. Fourth, paired-end reads were re-mapped to the sheep reference genome (Oar\_v4.0) using the align module of SpeedSeq v.0.1.2<sup>89</sup>.

In addition, sorted and duplicate-marked BAMs, which contain split reads and discordant read-pairs, were generated. SVs were then identified from the split reads and discordant pairs using LUMPY v.0.2.13<sup>90</sup>. CNVs were detected from the difference in read depth using CNVnator v.0.3.3<sup>91</sup>. The inferred breakpoints by LUMPY were genotyped using SVTyper v.0.1.4<sup>89</sup>. The variant types of SVs detected by the SpeedSeq framework are same as those by the GRIDSS pipeline. In these two pipelines, we generated non-uniquely mappable genomic regions for autosomes and X chromosomes, respectively, using SNPable (<http://lh3lh3.users.sourceforge.net/snpable.shtml>), and these regions were masked in the SV detection by the two methods described above.

To reduce the false-positive rate, SVs in both autosomes and X chromosomes from the four strategies (novoBreak, manta, GRIDSS and SpeedSeq) which meet the following seven criteria were retained: (i) at least three split reads (SR) or three spanning paired-end reads (PE) supporting the given SV event across all the samples; (ii) SVs with precise breakpoints by novoBreak (flag PRECISE); (iii) SVs passing the quality filters suggested by NovoBreak, manta, and GRIDSS (flag PASS); (iv) SVs with more than four supporting reads (flag SU) and without ambiguous breakpoints (flag IMPRECISE) in SpeedSeq; (v) SVs with lengths between 50 bp and 1 Mb; (vi) SVs without intersections between different variant types; and (vii) SVs identified by at least two pipelines. For each sample, the shared SVs detected at least by two of the four independent pipelines were merged using SURVIVOR v.1.0.6<sup>92</sup> with the parameters 500 2 1 1 0 50.

SVs were annotated based on their start positions using the package ANNOVAR v.2013-06-21<sup>84</sup>. Species-unbalanced SVs are defined as SVs which are unevenly distributed among different species. A two-sided Fisher's exact test was utilized to determine whether the distribution of each SV is uniform. The  $p$ -values for all the SVs were calculated with the Fisher.test function in R followed by the Benjamini-Hochberg false discovery rate (FDR) adjustment. SVs with FDR  $< 0.05$  were considered as species-unbalanced.

**SNPs and CNVs validation.** 74 randomly selected SNPs of 4–12 individuals were verified by PCR amplifications and Sanger sequencing. The primers used for the PCRs were designed with the software Primer Premier 5<sup>93</sup>. The PCR reactions were performed in a total volume of 25 μL, consisting of 12.5 μL 2× Taq MasterMix (Kangwei, Beijing, China), 2 μL (10 pmol/μL) reverse and forward primers, 1 μL template DNA (30 ng/μL) and 9.5 μL double-distilled water (ddH<sub>2</sub>O) under the reacting condition of initial denaturation at 95 °C for 3 min, 35 cycles for the following three steps, such as denaturation at 95 °C for 15 sec, annealing at 60 °C for 15 s, and extension at 72 °C for 30 s, with a final extension at 72 °C for 5 min. Following the PCR, the amplification products were sequenced on the Applied Biosystems 3730XL DNA Analyzer (Life Technologies, Carlsbad, CA, USA), and the sequencing peaks were checked with the software SEQMAN module of DNASTAR's LASERGENE<sup>94</sup>. Subsequently, genotypes obtained from the Sanger sequencing were compared with those inferred by the GATK pipelines (described above) from resequencing data for the same individuals.

Moreover, 14 randomly selected CNVs (e.g., seven deletions and seven duplications; Supplementary Data 3) were validated by quantitative real-time PCR (qPCR) or PCR. Primers were designed surrounding the deletions and within the duplications with the software Primer Premier 5 (Supplementary Data 3). Deletions were genotyped by PCR amplification and agarose gel electrophoresis. We measured the relative copy numbers of one deletion and all duplications using qPCR on the QuantStudio™ 6 Flex Real-Time PCR System (Life Technologies, Carlsbad, CA, USA) using SYBR Green kit (Promega, Madison, WI, USA). Following a previous study on sheep<sup>95</sup>, DGAT2 gene was used as the internal reference gene. qPCR reaction was in 25 μL volume consisting of 12.5 μL 2× SYBR Green qPCR Mix (Life Technologies, Carlsbad, CA, USA), 1 μL (10 pmol/μL) each primer (forward and reverse), 2 μL template DNA (30 ng/μL), and 8.5 μL ddH<sub>2</sub>O. The thermocycling condition includes an initial denaturation at 95 °C for 10 min, 40 cycles for the next three steps, such as denaturation at 95 °C for 15 s, annealing at 60 °C for 15 s and extension at 72 °C for 1 min, and a final extension at 72 °C for 10 min.



For qPCR, the  $\Delta\Delta C_T$  method<sup>96</sup> was applied to estimate the relative copy numbers. Equation for  $\Delta\Delta C_T$  value is  $\Delta\Delta C_T = [(C_{T\_segment} - C_{T\_DGAT2})_{target\ sample} - (C_{T\_segment} - C_{T\_DGAT2})_{control\ sample}]$ , where  $C_{T\_segment}$  is threshold cycle ( $C_T$ ) of target CNV segment and  $C_{T\_DGAT2}$  is the  $C_T$  of the internal reference gene<sup>96</sup>. We also measured the standard deviation of the  $\Delta\Delta C_T$  value using the formula:  $s = (s_1^2 + s_2^2)^{1/2}$ , where  $s_1$  is the variance of target  $C_T$  value (3 replications) and  $s_2$  is the variance of the reference  $C_T$  value (3 replications). The value of  $2 \times 2^{-\Delta\Delta C_T}$  between 1.5 and 3 were considered to most likely represent a normal copy number of 2, below 1.5 or above 3 are considered as deletions or duplications, respectively<sup>20</sup>. This was used to evaluate the concordance of calling results obtained from four SVs calling strategies and the relative copy number from the qPCR.

**Inference of demographic history.** We inferred past temporal change in  $N_e$  and population split times using the pairwise sequentially Markovian coalescent (PSMC) modeling (<http://github.com/lh3/psmc>) and SMC++ program (<https://github.com/popgenmethods/smcpp#masking>). We applied the parameters of a generation time ( $g$ ) of 3 years, neutral mutation rate ( $\mu$ ) =  $2.5 \times 10^{-8}$  per base pair per generation, a per-site filter of  $\geq 10$  reads, and no more than 25% of missing data<sup>97</sup>, including only autosomes from one high-coverage genomes ( $>18\times$ ) per species (PSMC, Supplementary Data 1) or three individuals per population or species (SMC++). We performed 1000 bootstrapping simulations to estimate the variance of  $N_e$ .

**Genomic diversity and population differentiation.** For each individual, genome-wide nucleotide diversity was calculated based on the set of high-quality SNPs ( $n = 6,558,545$ ) using Vcftools v0.1.13 with a window size of 200-kb. Genome-wide pairwise  $F_{ST}$  and  $d_{xy}$  genetic distance matrices between populations were estimated using in-house python scripts with a window size of 100-kb and a 20-kb step size. The matrices of pairwise distances were then plotted using the Corrplot package of R. In order to assess the genome-wide LD patterns of each species, we calculated  $r^2$  value using the program PopLDdecay v3.30<sup>98</sup> (<https://github.com/BGI-shenzhen/PopLDdecay>) with the default parameters and after filtering the sites with more than 10% missing genotypes among the individuals of each species cohort.

**Population genetic structure and phylogenetic reconstruction.** We implemented principal components analysis (PCA) using the Smartpca program<sup>99</sup> in the software EIGENSOFT v7.2.1<sup>100</sup> without outlier removal iteration (numoutlieriter: 0) but with the default settings of the other options. The Tracy-Widom test was used to determine the significance of the eigenvectors. The first two eigenvectors were plotted. We used the Ohana tool suite<sup>101</sup> to infer the global ancestry and the covariance structure of allele frequencies among the species. The number of ancestry components ( $K$ ) was set in a range from 2 to 11. For each  $K$ , we terminated the iteration when the likelihood improvement was smaller than 0.001 ( $-e$  0.001). We only reported the ones which reached the best likelihood for each  $K$ . Population trees at each  $K$  (Supplementary Fig. 12b) were plotted using the program Nemetree (<http://www.jade-cheng.com/trees/>).

The phylogenetic tree of the nine species was constructed using the maximum likelihood method implemented in the RAXML v8.2.3<sup>102</sup> with the multiple nucleotide substitution models. The tree was inferred based on the 12,837 protein-coding sequences (CDS) on autosomes and 513 CDS on X chromosome, separately. We used the protein-coding gene annotation file from NCBI ([ftp://ftp.ncbi.nlm.nih.gov/genomes/Ovis\\_aries/GFF/](ftp://ftp.ncbi.nlm.nih.gov/genomes/Ovis_aries/GFF/)). Only CDS with a length multiple of 3 were considered in the phylogenetic inference. The consensus trees (Supplementary Fig. 5) based on the whole genome were built on the concatenated CDSs of autosomes (33,868,497 bp), X chromosome (1,331,184 bp), and the whole mitogenomes (16,616 bp), respectively. Moreover, seventy-two haploidized whole-genome sequences for all the individuals were generated using the -doFasta3 option in ANGSD<sup>103</sup> (Fig. 2b and Supplementary Fig. 7), which uses the bases with the highest effective depth (EBD) and considers both mapping quality and scores for the bases<sup>104</sup>. To examine the impact of different assembly methods on the phylogenetic inference, we also tested the options of -doFasta 1 and -doFasta 2, which utilize the genomic sites by randomly selecting the base or selecting the base with the highest depth.

The preliminary tree for the optimization was constructed using the GTRCAT model in RAXML. Phylogenetic inference of autosomal and X chromosomal sequences was then implemented based on the first two codon positions and the third codon position of the whole concatenated coding sequence using the GTRGMMMA model in RAXML. The final trees after 200 bootstrapping replicates were generated using GTRCAT model in RAXML and returned to the preliminary tree labeled with bootstrap values. To clarify discordant coalescent events among different tracts in the genome, we split the whole genome into 1-Mb tracts, which result in 2598 non-overlapping windows, respectively. We inferred the ML trees using the GTRGMMMA model. Finally, trees were built of each 1-Mb windows (Supplementary Fig. 6). Numeration (classification and ranking) of trees was conducted using all.equal function in R package of Ape (analyses of phylogenetics and evolution) and plotted by in-house R scripts. The trees of each tract of autosomes and X chromosome in 1-Mb window were fitted and visualized by Densitree v2.0.1<sup>105</sup> (Fig. 2a). Mitochondrial sequences between sheep and goat were blasted using MEGA7<sup>106</sup>. Genomic coordinates of goat were transferred based

on locations of the sheep genome after trimming the poorly mapped sites. Finally, we merged the 73 mitochondrial sequences in the phylogenetic analysis with goat as the outgroup.

**Estimation of split time.** Divergence time was estimated locally based on each 1-Mb tracts across autosomes. We used the coalescent hidden Markov model (CoalHMM)<sup>23</sup>, a framework for demographic inference using a sequential Markov coalescent method, to estimate the split time with or without migrations among species. We first converted the pairwise sequence alignments using python scripts prepare-alignments.py (<https://github.com/birc-ah/coalhmm/tree/master/scripts/>). The I-CoalHMM and IM-CoalHMM models were then applied to the data set of 1-Mb tracts. The two models utilized the genome alignments of two species to calculate the time of speciation. In the I-CoalHMM model, a prior of split time and ancestral effective population size were needed, whereas in IM-CoalHMM model extra migration rates were also needed. The recombination rate was set as 1.5 cM/Mb<sup>107</sup>. We combined the nine pairwise alignments between species using 1-Mb splitting windows of the whole genomes for each pair and discarded the windows with  $>10\%$  missing bases. We filtered the time estimates for the windows using the following criteria: (i) a split time of below 1000 years or above 10,000 years for European mouflon and sheep, below 1000 years or above 20,000 years for Asiatic mouflon and sheep or below 10,000 years or above 10 million years for the divergence between the other seven pairs of species (Supplementary Figs. 9–11), (ii) a recombination rate below 0.1 cM/Mb or above 5 cM/Mb, and (iii) an ancestral effective population size below 5000 or above 1,000,000<sup>14</sup>.

**Migration events by TreeMix analysis.** To infer migration events among the eight species, we used TreeMix v1.13 to construct a ML tree with bighorn as the root using the “-noss” option to turn off the sample size correction, a window size (-K) of 500 SNPs (around 609-kb in this study) to account for the impact of LD, which is more than the average LD length of  $\sim 150$ -kb observed in sheep<sup>7</sup>. Blocks with 500 SNPs were resampled and 100 bootstrap replications were performed. We constructed the ML trees with 0–11 migration events and corresponding residuals. The proportions of explained variance (Supplementary Fig. 14) for the migration numbers were calculated using in-house scripts<sup>108</sup>.

**Gene flow among species.** To infer the ancestral alleles, genomic comparison between domestic sheep and domestic goat was carried out using the LAST v984 program (<http://last.cbrc.jp/>) (Supplementary Fig. 18). We aligned the sheep reference genome (Oar\_v4.0) to the goat reference genome (ASR.1) while masking the repeat regions. Only autosomal one-to-one orthologs were considered in the alignment between the two species using the lastal module with the parameters of -m 100 -E 0.05. To visualize the corresponding orthologs between species, a synteny plot was created using the circlize function in the R package. Samtools mpileup and Bcftools call were then used to call ancestral alleles. We merged these ancestral variants with the combined SNPs of all the 72 samples using Bcftools merge after indexing the two datasets. The combined data set was used to detect introgression among species.

To detect the potential gene flow among species, we conducted the ABBA-BABA test ( $D$ -statistics) based on two data panels: single high-depth genomes and high reliable SNPs among all the individuals. These two datasets can be collated with each other to reduce variants calling errors. For the first data panel, we performed the admixture analysis using ANGSD -doAbbababa 1 module with goat as the outgroup and the block size of 1,000,000 bp. For the second data panel, we examined the admixture among species using the qpDstats module of AdmixTools<sup>109</sup> and goat as the outgroup, which is a formal four-population test of admixture. Furthermore, we performed the three-population test using the qp3pop module of AdmixTools. The statistical significance of  $D$ -value was evaluated using a two-tailed  $Z$  test, with  $|Z\text{-score}| > 3$  to be significant<sup>110</sup>. We built the admixture graphs, fitted the graph parameters, and visualized the goodness of fit using admixturegraph<sup>111</sup> package in R.

**Inference of introgressed genomic regions.** To further localize the introgressed genomic regions across the whole-genome, a window-based Patterson's four-taxon  $D$ -statistic test  $D$  ( $P_1, P_2, P_3, O$ ) and modified  $f_4$ -statistic ( $f_4$ ) test with 100-kb length windows and 20-kb steps was performed using the methods of Martin et al.<sup>112</sup>.  $P_1$  was the reference population with no gene flow with  $P_3$  and is closer to  $P_2$  than  $P_3$ . Here, goat was used as the outgroup ( $O$ ), which was the ancestral population and shared derived alleles with populations  $P_1, P_2$ , and  $P_3$ . The significance level ( $p$ -value) of  $Z$ -transformed  $f_4$ -value was corrected by multiple testing using the Benjamini-Hochberg FDR method<sup>28</sup>. Windows with positive  $D$ -values and  $p$ -values (FDR adjusted)  $< 0.05$  were selected as the significantly introgressed regions, and the adjacent windows were merged into concatenated introgressed regions<sup>113</sup>.

We tested for genomic introgressions between different combinations of species.

(i)  $D$  (OUE, target; X, goat): The domestic population of Ouessant (OUE) serves as the reference population, the goat reference sequence was the outgroup, European mouflon, Asiatic mouflon or urial were the targets and X (bighorn, thinhorn, argali and snow sheep) was the to be tested source of introgression.

(ii) *D* (GMA, target; European mouflon, goat): We selected as reference the old and native Tibetan sheep (GMA) that has no potential gene flow with European mouflon and the targets were Ouessant in France, Mazekh in Azerbaijan, Makui, and Shal sheep in Iran.

(iii) *D* (GMA, target; Asiatic mouflon, goat): the targets were the domestic Mazekh, Makui, and Shal sheep.

(iv) *D* (OUE, Baidarak; snow sheep, goat): OUE from France was a suitable reference because its large distance to the range of snow sheep and Baidarak was the target.

(v) *D* (OUE, target; argali, goat): targets were domestic Tibetan sheep and Russian Baidarak.

(vi) *D* (OUE, target; urial goat): targets were domestic Mazekh, Makui, and Shal sheep. In addition, we calculated mean pairwise sequence divergence ( $d_{xy}$ ) and  $F_{ST}$  value between the target population (P2) and the test population (P3), as well as between the test population (P3) and the reference population (P1). Introgression but no shared ancestry reduces  $d_{xy}$  in the target regions<sup>112</sup>. Similarly, introgressed regions have lower divergence ( $F_{ST}$ ) than other regions.

**Dating introgression events.** We dated the time of ancient introgression using DATES<sup>114</sup> and Ancestry\_hmm program<sup>115</sup>. The software DATES computed the weighted LD statistic to infer the population admixture history, which has been developed for human datasets. However, because of the short generation time for sheep, the time estimates using DATES might be younger than expected. Thus, we also applied the Ancestry\_hmm program<sup>115</sup>, using phased data and only SNPs with at least two alleles in the reference populations and applying the following filters: (i) SNPs with allele frequency difference lower than 0.1 between the two reference populations; and (ii) SNPs with allele number less than 6 in a reference panel. Other parameters were set as default. We set the proportion of admixture ( $m$ ) according to admixture fraction obtained above by the  $f$ -statistics ( $f_d$ ) across the whole genomes. For dating the introgression from bighorn sheep, thinhorn sheep, snow sheep, or argali as a source of introgression (reference population 2) into Asiatic mouflon, we used urial as the ancestor (reference population 1). We applied a single pulse model for genotype data from each population and ran 100 bootstrap replicates using a block size of 5000 SNPs.

**Incomplete lineage sorting.** We calculated the probability of incomplete lineage sortings (ILSs) following the method in Huerta-Sánchez et al.<sup>116</sup>. Briefly, the expected length of a shared ancestral sequence is

$$L = 1/(r \times t). \quad (1)$$

The probability of a length of at least  $m$  follows from

$$1 - \text{GammaCDF}(k, \text{shape} = 2, r = 1/L), \quad (2)$$

in which GammaCDF is the Gamma distribution function,  $r$  is the recombination rate per generation per bp,  $m$  is the length of introgressed tracts, and  $t$  is the length of the two species branch since divergence. According to the theoretical expectation, we can exclude the possibility of common ancestral source when the detected length of tracts ( $m$ )  $> L$  or the probability of a length of at least  $m$  infinitely approaches zero. Here, we set recombination rate of  $1.5 \times 10^{-8}$ <sup>107</sup>, generation time of 4 years for Asiatic mouflon and urial<sup>117</sup>, and 3 years for domestic sheep<sup>118</sup>. We set divergence times of 2.3 Mya for snow sheep and Asiatic mouflon, 1.72 Mya for argali and Asiatic mouflon<sup>21</sup>, 2.42 Mya for the Pachycefiforms and the Moufloniforms (uriial, Asiatic mouflon, and European mouflon)<sup>1</sup>, 5–6 kya for European mouflon and domestic sheep<sup>24</sup>, ~11 kya for Asiatic mouflon and domestic sheep<sup>4</sup>, and ~1.26 Mya<sup>1</sup> for urial and domestic sheep.

**Functional annotation.** The genes which overlap with the concatenated introgressed regions detected by the modified  $f_d$ -value were annotated. We annotated and categorized the functions of genes using DAVIDv6.8<sup>119</sup> (<https://david.ncicrf.gov/>). FDR, Bonferroni and Benjamini–Hochberg adjusted  $p$ -values were estimated with  $p$ -value  $< 0.05$  as statistically significant. GO and KEGG pathway enrichment analyses were implemented using DAVIDv6.8<sup>119</sup> (<https://david.ncicrf.gov/>).

**Reporting summary.** Further information on research design is available in the Nature Research Reporting Summary linked to this article.

## Data availability

Raw sequencing data that support the findings of this study can be found in the NCBI SRA database under the BioProject (PRJNA764308) with the accession numbers SRR16036485, SRR16036486, SRR16036487, SRR16036488, SRR16036489, SRR16036490, SRR16036491, SRR16036492, SRR16036493, SRR16036494, SRR16036495, SRR16036496, SRR16036497, SRR16036498, SRR16036499, SRR16036500, SRR16036501, SRR16036502, SRR16036503, SRR16036504, SRR16036505, SRR16036506, SRR16036507, SRR16036508, SRR16036509, SRR16036510, SRR16036511, SRR16036512, SRR16036513, SRR16036514, SRR16036515, SRR16036516, SRR16036517, SRR16036518, and other data available under the BioProject PRJNA624020 and PRJNA645671 with the accession numbers SRR12397011, SRR12396918, SRR12

396917, SRR12396916, SRR11657538, SRR11657537, SRR11657536, SRR11657626, SRR11657631, SRR12397021, SRR12396955, SRR11657630, SRR12396952, SRR12396887, SRR12396886, SRR12396885, SRR12396883, SRR12396882, SRR12396881, SRR12396880, SRR12396951, SRR12396950, SRR11657640, SRR11657635, SRR11657636, SRR11657637, SRR11657638, SRR11657639, SRR11657641, SRR11657642, SRR11657500, SRR11657501, SRR11657502, SRR11657503, SRR11657504, SRR11657505, SRR11657506, and SRR11657507. Additional data such as raw image files and in-house scripts that support this study are available from the first authors upon request.

Received: 27 April 2021; Accepted: 27 October 2021;

Published online: 18 November 2021

## References

- Rezaei, H. R. et al. Evolution and taxonomy of the wild species of the genus *Ovis* (Mammalia, Artiodactyla, Bovidae). *Mol. Phylogenet. Evol.* **54**, 315–326 (2010).
- Zeder, M. A. Domestication and early agriculture in the Mediterranean Basin: origins, diffusion, and impact. *Proc. Natl. Acad. Sci. USA* **105**, 11597–11604 (2008).
- Wild, J. P. *ML Ryder: Sheep and Man* **58**, 142–142 (London: Duckworth, 1984).
- Chessa, B. et al. Revealing the history of sheep domestication using retrovirus integrations. *Science* **324**, 532–536 (2009).
- Woronozow, N. et al. Chromosomi dikich baranow i proisschojdenije domaschnich owjcz. *Lrroda* **3**, 74–81 (1972).
- Bunch, T. & Foote, W. Evolution of the 2n = 54 karyotype of domestic sheep (*Ovis aries*). *Ann. Genet. Sel. Anim.* **9**, 509–515 (1977).
- Alberto, F. J. et al. Convergent genomic signatures of domestication in sheep and goats. *Nat. Commun.* **9**, 1–9 (2018).
- Schröder, O. et al. Limited hybridization between domestic sheep and the European mouflon in Western Germany. *Eur. J. Wildl. Res.* **62**, 307–314 (2016).
- Bagirov, V. et al. Cytogenetic characteristic of *Ovis ammon ammon*, *O. Nivicola borealis* and their hybrids. *Сельскохозяйственная биология* **6**, 43–48 (2012).
- Jones, M. R. et al. Adaptive introgression underlies polymorphic seasonal camouflage in snowshoe hares. *Science* **360**, 1355–1358 (2018).
- Chen, N. et al. Whole-genome resequencing reveals world-wide ancestry and adaptive introgression events of domesticated cattle in East Asia. *Nat. Commun.* **9**, 2337 (2018).
- Figueiro, H. V. et al. Genome-wide signatures of complex introgression and adaptive evolution in the big cats. *Sci. Adv.* **3**, e1700299 (2017).
- Gopalakrishnan, S. et al. Interspecific gene flow shaped the evolution of the genus *Canis*. *Curr. Biol.* **28**, 3441–3449.e5 (2018).
- Wu, D. D. et al. Pervasive introgression facilitated domestication and adaptation in the *Bos* species complex. *Nat. Ecol. Evol.* **2**, 1139–1145 (2018).
- Barbato, M. et al. Genomic signatures of adaptive introgression from European mouflon into domestic sheep. *Sci. Rep.* **7**, 7623 (2017).
- Hu, X. J. et al. The genome landscape of Tibetan sheep reveals adaptive introgression from argali and the history of early human settlements on the Qinghai-Tibetan plateau. *Mol. Biol. Evol.* **36**, 283–303 (2019).
- Li, X. et al. Whole-genome resequencing of wild and domestic sheep identifies genes associated with morphological and agronomic traits. *Nat. Commun.* **11**, 2815 (2020).
- Naval-Sanchez, M. et al. Sheep genome functional annotation reveals proximal regulatory elements contributed to the evolution of modern breeds. *Nat. Commun.* **9**, 859 (2018).
- Deng, J. et al. Paternal origins and migratory episodes of domestic sheep. *Curr. Biol.* **30**, 4085–4095.e6 (2020).
- Zhou, Y. et al. Genome-wide copy number variant analysis reveals variants associated with 10 diverse production traits in Holstein cattle. *BMC Genomics* **19**, 314 (2018).
- Bunch, T. D., Wu, C., Zhang, Y. P. & Wang, S. Phylogenetic analysis of snow sheep (*Ovis nivicola*) and closely related taxa. *J. Hered.* **97**, 21–30 (2006).
- Ciani, E. et al. On the origin of European sheep as revealed by the diversity of the Balkan breeds and by optimizing population-genetic analysis tools. *Genet. Sel. Evol.* **52**, 25 (2020).
- Mailund, T. et al. A new isolation with migration model along complete genomes infers very different divergence processes among closely related great ape species. *PLoS Genet.* **8**, e1003125 (2012).
- Vigne, J. D. Zooarchaeology and the biogeographical history of the mammals of Corsica and Sardinia since the last ice age. *Mamm. Rev.* **22**, 87–96 (1992).
- Larson, G. et al. Current perspectives and the future of domestication studies. *Proc. Natl. Acad. Sci. USA* **111**, 6139 (2014).

26. Nielsen, R. et al. Tracing the peopling of the world through genomics. *Nature* **541**, 302–310 (2017).
27. Mason, I. A *World Dictionary of Livestock Breeds, Types and Varieties* (CAB International, Wallingford, UK, 1996).
28. Benjamini, Y. & Hochberg, Y. Controlling the false discovery rate: a practical and powerful approach to multiple testing. *J. R. Stat. Soc. Ser. B* **57**, 289–300 (1995).
29. Yang, H. et al. Identification and profiling of microRNAs from ovary of estrous Kazakh sheep induced by nutritional status in the anestrus season. *Anim. Reprod. Sci.* **175**, 18–26 (2016).
30. Posbergh, C. J., Thonney, M. L. & Huson, H. J. P5017 Identifying genetic regions to spring ewes to lamb out of season. *J. Anim. Sci.* **94**, 123–124 (2016).
31. Peng, W. F. et al. A genome-wide association study reveals candidate genes for the supernumerary nipple phenotype in sheep (*Ovis aries*). *Anim. Genet.* **48**, 570–579 (2017).
32. Jia, C. et al. Identification of genetic loci associated with growth traits at weaning in yak through a genome-wide association study. *Anim. Genet.* **51**, 300–305 (2020).
33. Liu, G. et al. Expression profiling reveals genes involved in the regulation of wool follicle bulb regression and regeneration in sheep. *Int. J. Mol. Sci.* **16**, 9152–9166 (2015).
34. Tarsani, E. et al. Discovery and characterization of functional modules associated with body weight in broilers. *Sci. Rep.* **9**, 9125 (2019).
35. Huang, D. et al. Identification of the mouse and rat orthologs of the gene mutated in Usher syndrome type IIA and the cellular source of *USH2A* mRNA in retina, a target tissue of the disease. *Genomics* **80**, 195–203 (2002).
36. Iwama, E. et al. Cancer-related *PRUNE2* protein is associated with nucleotides and is highly expressed in mature nerve tissues. *J. Mol. Neurosci.* **44**, 103–114 (2011).
37. Wallace, R. M., Pohler, K. G., Smith, M. F. & Green, J. A. Placental PAGs: gene origins, expression patterns, and use as markers of pregnancy. *Reproduction* **149**, R115–R126 (2015).
38. Cao, Y. H. et al. Historical introgression from wild relatives enhanced climatic adaptation and resistance to pneumonia in sheep. *Mol. Biol. Evol.* **38**, 838–855 (2020).
39. Al Kalaldehy, M., Gibson, J., Lee, S. H., Gondro, C. & van der Werf, J. H. J. Detection of genomic regions underlying resistance to gastrointestinal parasites in Australian sheep. *Genet. Sel. Evol.* **51**, 37 (2019).
40. Wong, D. et al. Genomic mapping of the MHC transactivator *CIITA* using an integrated ChIP-seq and genetical genomics approach. *Genome Biol.* **15**, 494 (2014).
41. Wang, W. et al. Deep genome resequencing reveals artificial and natural selection for visual deterioration, plateau adaptability and high prolificacy in Chinese domestic sheep. *Front. Genet.* **10**, 300–300 (2019).
42. Bouloy, M. & Weber, F. Molecular biology of rift valley Fever virus. *Open Virol. J.* **4**, 8–14 (2010).
43. Liu, L. L., Fang, C. & Liu, W. J. Identification on novel locus of dairy traits of Kazakh horse in Xinjiang. *Gene* **677**, 105–110 (2018).
44. Taye, M. et al. Exploring evidence of positive selection signatures in cattle breeds selected for different traits. *Mamm. Genome* **28**, 528–541 (2017).
45. Yurchenko, A. A. et al. High-density genotyping reveals signatures of selection related to acclimation and economically important traits in 15 local sheep breeds from Russia. *BMC Genomics* **20**, 294 (2019).
46. Jin, Y. et al. Detection of insertions/deletions within *SIRT1*, *SIRT2* and *SIRT3* genes and their associations with body measurement traits in cattle. *Biochem. Genet.* **56**, 663–676 (2018).
47. Yuan, Z. et al. Selection signature analysis reveals genes associated with tail type in Chinese indigenous sheep. *Anim. Genet.* **48**, 55–66 (2017).
48. Häkkelien, A. M. et al. The regulatory landscape of osteogenic differentiation. *Stem Cells* **32**, 2780–2793 (2014).
49. Zhang, X. et al. Association analysis of polymorphism in the *NR6A1* gene with the lumbar vertebrae number traits in sheep. *Genes Genom.* **41**, 1165–1171 (2019).
50. Ehrmann, I. et al. An ancient germ cell-specific RNA-binding protein protects the germline from cryptic splice site poisoning. *eLife* **8**, e39304 (2019).
51. Cardoso, T. F. et al. RNA-seq based detection of differentially expressed genes in the skeletal muscle of Duroc pigs with distinct lipid profiles. *Sci. Rep.* **7**, 40005 (2017).
52. Petersen, J. L. et al. Genome-wide analysis reveals selection for important traits in domestic horse breeds. *PLoS Genet* **9**, e1003211–e1003211 (2013).
53. Taye, M. et al. Exploring the genomes of East African Indicine cattle breeds reveals signature of selection for tropical environmental adaptation traits. *Cogent Food Agric.* **4**, 1552552 (2018).
54. Li, Y. et al. Heat stress-responsive transcriptome analysis in the liver tissue of Hu sheep. *Genes* **10**, 395 (2019).
55. Lyon, M. S. & Milligan, C. Extracellular heat shock proteins in neurodegenerative diseases: new perspectives. *Neurosci. Lett.* **711**, 134462 (2019).
56. Yang, J. et al. Whole-genome sequencing of native sheep provides insights into rapid adaptations to extreme environments. *Mol. Biol. Evol.* **33**, 2576–2592 (2016).
57. Atlija, M., Arranz, J.-J., Martínez-Valladares, M. & Gutiérrez-Gil, B. Detection and replication of QTL underlying resistance to gastrointestinal nematodes in adult sheep using the ovine 50K SNP array. *Genet. Sel. Evol.* **48**, 4 (2016).
58. Nakamura, H. et al. Identification of a human homolog of the *Drosophila* neuralized gene within the 10q25.1 malignant astrocytoma deletion region. *Oncogene* **16**, 1009–1019 (1998).
59. Zong, S. et al. Association of polymorphisms in heat shock protein 70 genes with the susceptibility to noise-induced hearing loss: a meta-analysis. *PLoS ONE* **12**, e0188195 (2017).
60. Lv, F. H. et al. Mitogenomic meta-analysis identifies two phases of migration in the history of Eastern Eurasian sheep. *Mol. Biol. Evol.* **32**, 2515–2533 (2015).
61. Tarekeng, G. M. et al. Ethiopian indigenous goats offer insights into past and recent demographic dynamics and local adaptation in sub-Saharan African goats. *Evol. Appl.* **14**, 1716–1731 (2021).
62. Fang, Y. et al. Genome-wide detection of runs of homozygosity in Laiwu pigs revealed by sequencing data. *Front. Genet.* **12**, 629966–629966 (2021).
63. Benjelloun, B. et al. An evaluation of sequencing coverage and genotyping strategies to assess neutral and adaptive diversity. *Mol. Ecol. Resour.* **19**, 1497–1515 (2019).
64. Zhang, J. et al. Effect of domestication on the genetic diversity and structure of *Saccharina japonica* populations in China. *Sci. Rep.* **7**, 42158 (2017).
65. Demirci, S. et al. Mitochondrial DNA diversity of modern, ancient and wild sheep (*Ovis gmelinii anatolica*) from Turkey: new insights on the evolutionary history of sheep. *PLoS ONE* **8**, e81952 (2013).
66. Nadler, C. F., Hoffmann, R. S. & Woolf, A. G-band patterns as chromosomal markers, and the interpretation of chromosomal evolution in wild sheep (*Ovis*). *Experientia* **29**, 117–119 (1973).
67. Sanna, D. et al. The first mitogenome of the Cyprus mouflon (*Ovis gmelini ophion*): new insights into the phylogeny of the genus *Ovis*. *PLoS ONE* **10**, e0144257 (2015).
68. Poplin, F. Origine du Mouflon de Corse dans une nouvelle perspective paléontologique: par marronnage. *Ann. Genet. Sel. Anim.* **11**, 133–143 (1979).
69. Vigne, J. D., Carrère, I., Brioso, F. & Guilaine, J. The early process of mammal domestication in the Near East: new evidence from the pre-Neolithic and pre-Pottery Neolithic in Cyprus. *Curr. Anthropol.* **52**, S255–S271 (2011).
70. Yang, Y. et al. Draft genome of the Marco Polo Sheep (*Ovis ammon polii*). *GigaScience* **6**, 1–7 (2017).
71. Carling, M. D., Lovette, I. J. & Brumfield, R. T. Historical divergence and gene flow: coalescent analyses of mitochondrial, autosomal and sex-linked loci in *Passerina Buntings*. *Evolution* **64**, 1762–1772 (2010).
72. Zheng, Z. et al. The origin of domestication genes in goats. *Sci. Adv.* **6**, eaaz5216 (2020).
73. Fan, R. et al. Genomic analysis of the domestication and post-Spanish conquest evolution of the llama and alpaca. *Genome Biol.* **21**, 159 (2020).
74. An, X. et al. Two mutations in the 5'-flanking region of the *KITLG* gene are associated with litter size of dairy goats. *Anim. Genet.* **46**, 308–311 (2015).
75. Zhang, J. et al. Expression and polymorphisms of *KITLG* gene and their association with litter size in sheep (*Ovis aries*). *J. Agric. Biotechnol.* **25**, 893–900 (2017).
76. Pan, Y. et al. Indel mutations of sheep *PLAG1* gene and their associations with growth traits. *Anim. Biotechnol.* **7**, 1–7 (2021).
77. Li, Y. et al. Mutation-388 C>G of NR5A1 gene affects litter size and promoter activity in sheep. *Anim. Reprod. Sci.* **196**, 19–27 (2018).
78. Hunter, P. The genetics of domestication: research into the domestication of livestock and companion animals sheds light both on their “evolution” and human history. *EMBO Rep.* **19**, 201–205 (2018).
79. Fedosenko, A. K. & Blank, D. A. *Ovis ammon*. *Mamm. Species* **2005**, 1–15 (2005).
80. Sambrook, J. & Russell, D. *Molecular Cloning: A Laboratory Manual* (Cold Spring Harbor Laboratory Press, New York, 2001).
81. Li, H. & Durbin, R. Fast and accurate short read alignment with Burrows-Wheeler transform. *Bioinformatics* **25**, 1754–1760 (2009).
82. McKenna, A. et al. The Genome Analysis Toolkit: a MapReduce framework for analyzing next-generation DNA sequencing data. *Genome Res.* **20**, 1297–1303 (2010).
83. Chang, C. C. et al. Second-generation PLINK: rising to the challenge of larger and richer datasets. *Gigascience* **4**, 7 (2015).
84. Wang, K., Li, M. & Hakonarson, H. ANNOVAR: functional annotation of genetic variants from high-throughput sequencing data. *Nucleic Acids Res.* **38**, e164 (2010).
85. Delaneau, O. & Marchini, J. Integrating sequence and array data to create an improved 1000 Genomes Project haplotype reference panel. *Nat. Commun.* **5**, 3934 (2014).



86. Chong, Z. et al. novoBreak: local assembly for breakpoint detection in cancer genomes. *Nat. Methods* **14**, 65–67 (2017).
87. Chen, X. et al. Manta: rapid detection of structural variants and indels for germline and cancer sequencing applications. *Bioinformatics* **32**, 1220–1222 (2016).
88. Cameron, D. L. et al. GRIDSS: sensitive and specific genomic rearrangement detection using positional de Bruijn graph assembly. *Genome Res.* **27**, 2050–2060 (2017).
89. Chiang, C. et al. SpeedSeq: ultra-fast personal genome analysis and interpretation. *Nat. Methods* **12**, 966–968 (2015).
90. Layer, R. M., Chiang, C., Quinlan, A. R. & Hall, I. M. LUMPY: a probabilistic framework for structural variant discovery. *Genome Biol.* **15**, R84 (2014).
91. Abyzov, A., Urban, A. E., Snyder, M. & Gerstein, M. CNVnator: an approach to discover, genotype, and characterize typical and atypical CNVs from family and population genome sequencing. *Genome Res.* **21**, 974–984 (2011).
92. Jeffares, D. C. et al. Transient structural variations have strong effects on quantitative traits and reproductive isolation in fission yeast. *Nat. Commun.* **8**, 14061 (2017).
93. Lalitha, S. Primer premier 5. *Biotech. Softw. Internet Rep.* **1**, 270–272 (2000).
94. Swindell, S. R. & Plasterer, T. N. SEQMAN. Contig assembly. *Methods Mol. Biol.* **70**, 75–89 (1997).
95. Yuan, C. et al. A global analysis of CNVs in Chinese indigenous fine-wool sheep populations using whole-genome resequencing. *BMC Genomics* **22**, 78 (2021).
96. Schmittgen, T. D. & Livak, K. J. Analyzing real-time PCR data by the comparative CT method. *Nat. Protoc.* **3**, 1101–1108 (2008).
97. Nadachowska-Brzyska, K., Burri, R., Smeds, L. & Ellegren, H. PSMC analysis of effective population sizes in molecular ecology and its application to black-and-white *Ficedula flycatchers*. *Mol. Ecol.* **25**, 1058–1072 (2016).
98. Zhang, C., Dong, S. S., Xu, J. Y., He, W. M. & Yang, T. L. PopLDdecay: a fast and effective tool for linkage disequilibrium decay analysis based on variant call format files. *Bioinformatics* **35**, 1786–1788 (2019).
99. Patterson, N., Price, A. L. & Reich, D. Population structure and eigenanalysis. *PLoS Genet.* **2**, e190 (2006).
100. Price, A. L., Zaitlen, N. A., Reich, D. & Patterson, N. New approaches to population stratification in genome-wide association studies. *Nat. Rev. Genet.* **11**, 459–463 (2010).
101. Cheng, J. Y., Stern, A. J., Racimo, F., & Nielsen, R. Detecting selection in multiple populations by modelling ancestral admixture components. *Mol. Biol. Evol.* msab294, <https://doi.org/10.1093/molbev/msab294> (2021).
102. Stamatakis, A. RAXML version 8: a tool for phylogenetic analysis and post-analysis of large phylogenies. *Bioinformatics* **30**, 1312–1313 (2014).
103. Korneliussen, T. S., Albrechtsen, A. & Nielsen, R. ANGSD: analysis of next generation sequencing data. *BMC Bioinformatics* **15**, 356 (2014).
104. Wang, Y., Lu, J., Yu, J., Gibbs, R. A. & Yu, F. An integrative variant analysis pipeline for accurate genotype/haplotype inference in population NGS data. *Genome Res.* **23**, 833–842 (2013).
105. Bouckaert, R. R. DensiTree: making sense of sets of phylogenetic trees. *Bioinformatics* **26**, 1372–1373 (2010).
106. Kumar, S., Stecher, G. & Tamura, K. MEGA7: molecular evolutionary genetics analysis version 7.0 for bigger datasets. *Mol. Biol. Evol.* **33**, 1870–1874 (2016).
107. Petit, M. et al. Variation in recombination rate and its genetic determinism in sheep populations. *Genetics* **207**, 767–784 (2017).
108. Pickrell, J. K. & Pritchard, J. K. Inference of population splits and mixtures from genome-wide allele frequency data. *PLoS Genet.* **8**, e1002967 (2012).
109. Patterson, N. et al. Ancient admixture in human history. *Genetics* **192**, 1065–1093 (2012).
110. Durand, E. Y., Patterson, N., Reich, D. & Slatkin, M. Testing for ancient admixture between closely related populations. *Mol. Biol. Evol.* **28**, 2239–2252 (2011).
111. Leppala, K., Nielsen, S. V. & Mailund, T. admixturegraph: an R package for admixture graph manipulation and fitting. *Bioinformatics* **33**, 1738–1740 (2017).
112. Martin, S. H., Davey, J. W. & Jiggins, C. D. Evaluating the use of ABBA-BABA statistics to locate introgressed loci. *Mol. Biol. Evol.* **32**, 244–257 (2015).
113. Teng, H. et al. Population genomics reveals speciation and introgression between brown Norway rats and their sibling species. *Mol. Biol. Evol.* **34**, 2214–2228 (2017).
114. Loh, P. R. et al. Inferring admixture histories of human populations using linkage disequilibrium. *Genetics* **193**, 1233–1254 (2013).
115. Corbett-Detig, R. & Nielsen, R. A hidden markov model approach for simultaneously estimating local ancestry and admixture time using next generation sequence data in samples of arbitrary ploidy. *PLoS Genet.* **13**, e1006529 (2017).
116. Huerta-Sanchez, E. et al. Altitude adaptation in Tibetans caused by introgression of Denisovan-like DNA. *Nature* **512**, 194–197 (2014).
117. Guerrini, M. et al. Molecular DNA identity of the mouflon of Cyprus (*Ovis orientalis ophion*, Bovidae): near Eastern origin and divergence from Western Mediterranean conspecific populations. *System. Biodivers.* **13**, 472–483 (2015).
118. Zhao, Y. X. et al. Genomic reconstruction of the history of native sheep reveals the peopling patterns of nomads and the expansion of early pastoralism in East Asia. *Mol. Biol. Evol.* **34**, 2380–2395 (2017).
119. Huang da, W., Sherman, B. T. & Lempicki, R. A. Systematic and integrative analysis of large gene lists using DAVID bioinformatics resources. *Nat. Protoc.* **4**, 44–57 (2009).

## Acknowledgements

This study was financially supported by grants from the National Key Research and Development Program-Key Projects of International Innovation Cooperation between Governments (2017YFE0117900), the External Cooperation Program of Chinese Academy of Sciences (152111KYSB20190027), the National Natural Science Foundation of China (Nos. 31661143014, 31825024, and 31972527), and the Second Tibetan Plateau Scientific Expedition and Research Program (STEP) (No. 2019QZKK0501). We thank Ming-Shan Wang, Sheng Wang, Hua-Jing Teng, Da-Qi Yu, Peter Wilton, and Débora YC Brandt for their technical help with the statistical analysis. We express our thanks to the owners of the sheep for donating samples (Supplementary Data 1). Thanks are also due to a number of persons for their help during sample collection.

## Author contributions

M.-H.L. conceived the study. M.-H. L. and R.N. supervised the study. Z.-H.C. and Y.-X.X. conducted the laboratory work. Z.-H.C., X.-L.X., and G.-J.L. contributed to the data analysis. D.-F.W. and D.A.G. provided the help for coding. X.-L.X. and G.-J.L. performed the analysis of SVs. Z.-H.C., X.-L.X., Y.-X.X., D.W.C., A.E., J.A.L., R.N., and M.-H.L. wrote or revised the paper. K.P., I.A., D.W.C., J. K., M.N., and V.R. contributed samples or provided help during the sample collection. All the authors reviewed and approved the final manuscript.

## Competing interests

The authors declare no competing interests.

## Ethics statement

All animal work was conducted according to a permit (No. IOZ13015) approved by the Committee for Animal Experiments of the Institute of Zoology, Chinese Academy of Sciences (CAS), China. For domestic sheep, animal sampling was also approved by local authorities where the samples were taken.

## Additional information

**Supplementary information** The online version contains supplementary material available at <https://doi.org/10.1038/s42003-021-02817-4>.

**Correspondence** and requests for materials should be addressed to Rasmus Nielsen or Meng-Hua Li.

**Peer review information** *Communications Biology* thanks the anonymous reviewers for their contribution to the peer review of this work. Primary Handling Editors: Luciano Matzkin and Caitlin Karniski.

**Reprints and permission information** is available at <http://www.nature.com/reprints>

**Publisher's note** Springer Nature remains neutral with regard to jurisdictional claims in published maps and institutional affiliations.



**Open Access** This article is licensed under a Creative Commons Attribution 4.0 International License, which permits use, sharing, adaptation, distribution and reproduction in any medium or format, as long as you give appropriate credit to the original author(s) and the source, provide a link to the Creative Commons license, and indicate if changes were made. The images or other third party material in this article are included in the article's Creative Commons license, unless indicated otherwise in a credit line to the material. If material is not included in the article's Creative Commons license and your intended use is not permitted by statutory regulation or exceeds the permitted use, you will need to obtain permission directly from the copyright holder. To view a copy of this license, visit <http://creativecommons.org/licenses/by/4.0/>.

© The Author(s) 2021